ACS Energy LETTERS

http://pubs.acs.org/journal/aelccp

FOCUS REVIEW

Heterogeneous Electrocatalysts for Metal–CO_2 Batteries and CO_2 Electrolysis

Jianda Wang, Barbara Marchetti, Xiao-Dong Zhou,* and Shuya Wei*

Cite This: *ACS Energy Lett.* 2023, 8, 1818–1838

Read Online

ACCESS | Metrics & More | Article Recommendations

ABSTRACT: Heterogeneous electrocatalysis is one of the most promising ways to advance the development of metal–CO_2 batteries and CO_2 electrolysis technologies. Although both research areas rely upon efficient electrochemical reduction of CO_2, to date the respective research has been largely carried out independently. This Focus Review introduces the latest innovative design strategies toward heterogeneous electrocatalysts applied for both metal–CO_2 batteries and CO_2 electrolysis. The structural design of various categories of catalysts, their synthesis methods, and electrocatalytic reactions are discussed in detail. The review also presents a discussion of the fundamental reaction mechanisms active for both applications. Finally, we will reflect on the challenges and new opportunities for each category of electrocatalysts. We hope to provide researchers a more comprehensive understanding of the design of high-performing electrocatalysts to advance both metal–CO_2 batteries and CO_2 electrolysis technologies.

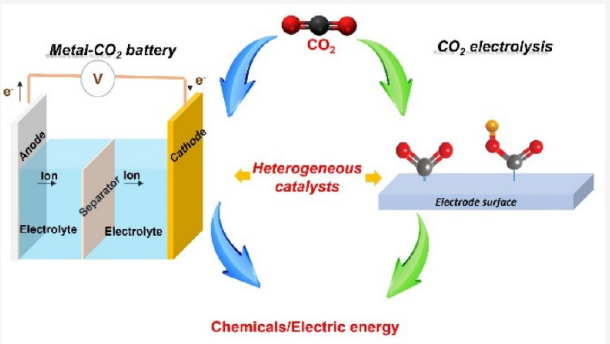

The excessive emissions of carbon dioxide (CO_2) by anthropogenic activities, such as heavy exploitation of fossil fuels and deforestation, have been linked to urgent social and environmental problems, i.e., ocean acidification and global warming.[1−5] In the absence of effective solutions, it is predicted that the atmospheric concentration of CO_2 will double within the next century. Thus, a great deal of current research is devoted to developing stable and efficient methods to capture and convert excess atmospheric CO_2 into other useful chemicals.[6−15] A notable example of CO_2 capture is the liquid solvent capture method. Such a method may employ pyridinium-containing amide-based poly(ionic liquid)s (PAP-ILs), which have the capability of adsorbing large amounts of atmospheric CO_2, thus allowing storing it underground for extended time.[16] However, low efficiency and high operating costs, as well as the potential emission of harmful solvent waste, present inevitable challenges to the large-scale application of this technology. Multiple challenges still need to be overcome to find a high-efficiency and environment-friendly method to achieve this goal.[17−25] Fortunately, researchers found that CO_2 electroreduction reaction (CO_2ER) offers a promising way out of this dilemma, owing to its precisely regulated reaction rates and products.[26−35] Recent developments in technologies for CO_2 electroconversion indicate feasible pathways to produce value-added chemicals.[36−39] Among these applications, metal–CO_2 batteries and CO_2 electrolysis are promising means to capture CO_2 while storing electric energy or producing useful fuels or chemicals.[40,41,50,42−49]

Metal–CO_2 batteries (metal = Li, Na, Zn, or Al) have received considerable attention as a means to both facilitate electroreduction of CO_2 into different discharge products and store electrical energy.[51−54] Li/Na–CO_2 batteries have the potential to be commercialized primarily for their high theoretical energy density and inexpensive electrode materials. Furthermore, recent developments of Zn/Al–CO_2 batteries have also shown promising results. CO_2 electrolysis is another important application of CO_2ER. This entails adsorbing CO_2 on the electrode surface and reducing it to different possible carbonous products (carbon monoxide, hydrocarbons, etc.). The advantage of this approach is that the formation of final products can be controlled under different conditions, potentially providing a selected subset of key chemical products.[55−57] In both applications, the basic premise is that an initial fast and efficient electron transfer occurs from an electron donor to the adsorbed CO_2; such electron transfer

Received: October 30, 2022
Accepted: March 9, 2023
Published: March 20, 2023

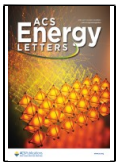

promotes cleavage or weakening of the C=O bonds, thus activating CO_2 toward the ensuing electrochemical processes. Generally, in metal−CO_2 batteries, the CO_2ER simply leads to the formation of C or CO. On the other hand, in general electrocatalysis, CO_2 may be reduced into a vast array of products, ranging from CO, to ethylene, formic acid, methylglyoxal, and many more. This prospect makes CO_2ER very attractive and versatile, as it may open the doorway to sustainable, green production of several added-value chemicals. Nonetheless, both metal−CO_2 batteries and CO_2 electrolysis technologies are facing a fundamental challenge; as CO_2 is one of the most stable molecules, activation of C=O is particularly difficult to achieve and is associated with extremely slow kinetics (reduced molar Gibbs free energy of CO_2: 213.8 $J \cdot mol^{-1} \cdot K^{-1}$ at 298 K). Additional technical challenges arise from the poor cycling performance and high overpotential of the metal−CO_2 battery cell, while CO_2 electrolysis often faces unsatisfactory selectivity. To date, such limitations are often considered a hindrance to further development of these technologies and their large-scale deployment.[58] However, continuous advances in the design of heterogeneous electrocatalysts showed a promising way to tackle these challenges, for both facilitating the process of capturing CO_2 and achieving high-efficiency CO_2ER.

Heterogeneous electrocatalysts have been commonly used in both metal−CO_2 batteries and CO_2 electrolysis applications to enhance the reaction kinetics of CO_2. Both applications require heterogeneous electrocatalysts to break C=O bond(s) in CO_2 as the initial step and to form other carbon species.

Heterogeneous electrocatalysts have been commonly used in both metal−CO_2 batteries and CO_2 electrolysis applications to enhance the reaction kinetics of CO_2ER. Both applications require heterogeneous electrocatalysts to facilitate the activation of CO_2 and cleavage of the C=O bond(s). In metal−CO_2 batteries, heterogeneous electrocatalysts are applied in the cathode to control the formation/decomposition of discharge product and facilitate CO_2/ion transfer.[59−64] In CO_2 electrolysis, heterogeneous electrocatalysts play an essential role in CO_2 adsorption and the formation of the reduced intermediates.[65] Several excellent reviews have focused on the role of electrocatalysts in each of the two applications. For example, Mu et al. summarized the mechanism and design strategies of electrocatalysts for metal−CO_2 batteries.[40] Manthiram and co-workers provided an overview of heterogeneous molecular electrocatalysts for CO_2 electrolysis, including the fundamental mechanistic aspects underlying CO_2ER.[11] However, as far as heterogeneous electrocatalysis is concerned, the connection between metal−CO_2 batteries and CO_2 electrolysis applications has not been analyzed to a large extent. Given that both technologies rely on a common initial reaction step, we believe that the heterogeneous catalysis underlying both metal−CO_2 batteries and CO_2 electrolysis has deeper interrelations, which should be appraised for enhancing the efficiencies of both applications.[66] Therefore, in this Focus Review, we first examine several categories of heterogeneous electrocatalysts that can be applied for both metal−CO_2 battery and CO_2 electrolysis applications (Scheme 1).

We introduce and assess the latest progress in a variety of heterogeneous electrocatalysts and their corresponding synthetic methods. These will include the synthesis and performance of carbon-based electrocatalysts, as well as noble metal-based and transition metal compound-based electrocatalysts, single-atom catalysts, and organic polymers (Figure 1). Second, we focus on the reaction mechanisms and strategies to improve cell efficiencies with the aim of providing guidelines for future design of improved electrocatalysts for CO_2 electrolysis and CO_2−metal batteries. Finally, we discuss the remaining challenges in these two applications and provide a future outlook in detail. We hope this Focus Review offers a comprehensive understanding of recent advances in heterogeneous electrocatalysts to boost the development of both CO_2 electrolysis technologies and CO_2−metal batteries.

CARBON-BASED ELECTROCATALYSTS

The different types of electrocatalysts for metal−CO_2 batteries and their electrocatalytic performance are summarized in Table 1. Table 2 summarizes the electrochemical performance of different types of electrocatalysts used for CO_2 reduction. Among these, carbon-based electrocatalysts have aroused significant interest as cost-effective, metal-free catalysts with high electrical conductivity, tunable morphological structures, and high surface areas. At first, graphene (G) and carbon nanotubes (CNT) are attractive materials due to their superior electronic properties and unique structures. However, reversible decomposition of the discharge products is still a major challenge for these carbon-based electrocatalysts.[82] Furthermore, the accumulation of the discharge products onto the cathode surface may yield to coverage of active sites and thus affect the cycle stability of the battery. A deeper understanding of the electronic, structural, and morphological aspects of carbon-based electrocatalysts as well as the availability of active sites is essential for improving their catalytic properties. Heteroatom doping is an effective strategy to further improve the electrocatalytic performance of carbon-based electrocatalysts. Among others, nitrogen (N) is a common doping element for carbon. Chen et al. reported that CO_2-activated nitrogen-doped carbon/graphene oxide (CA-NG/RGO) showed improved CO_2ER kinetics and discharge−charge performance of Li−CO_2 battery.[67] Figure 2b summarizes the synthesis of CA-NG/RG; this relies on a rather simple, yet elegant method to prepare the catalyst with pyrrolic and pyridinic N sites by CO_2 activation. The resulting catalyst yields to the reversible formation and decomposition of the discharge product (Li_2CO_3). During the decomposition, pyridinic-N and pyrrolic-N can strongly bind to Li and Li_2CO_3. Analysis of the electronic charge distributions showed decreased charge densities between the Li_2 and O atoms, such as those typically involved in bond elongation processes. This is indicative of weakened Li_2−O bonds, which result in faster kinetics for decomposition of Li_2CO_3. This was also confirmed by lower decomposition barriers predicted on the pyridinic/pyrrolic-N active sites cf. graphitic-N (or C graphene) sites, which further corroborates the better performance.

Another imposing way to improve electrocatalytic performance of carbon-based materials is to facilitate the charge transfer and ion/gas diffusion at the cathode. Xiao et al. developed a single-step chemical vapor deposition (CVD) method to

https://doi.org/10.1021/acsenergylett.2c02445
ACS Energy Lett. 2023, 8, 1818−1838

Scheme 1. Connection of Heterogeneous Electrocatalysts and Corresponding Mechanism between Metal−CO_2 Batteries and CO_2 Electrolysis Applications

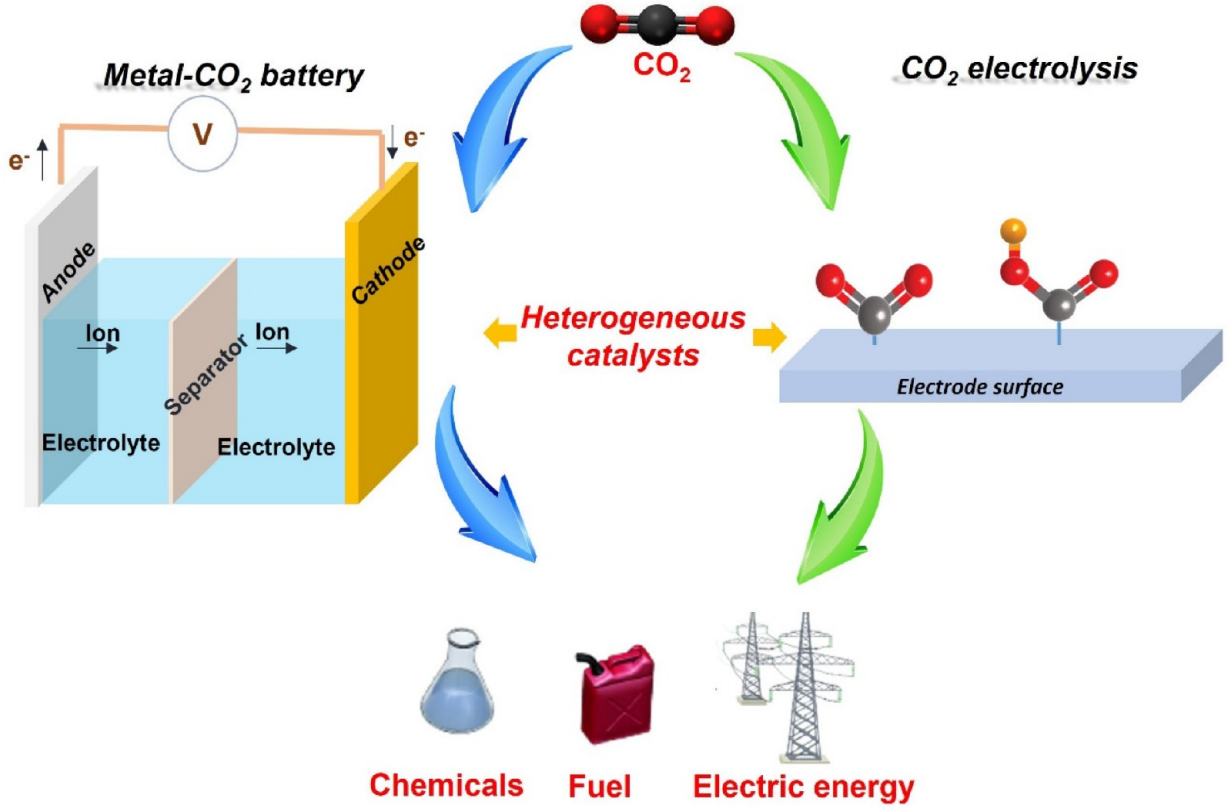

synthesize N-doped CNT/graphene (NCNT/G) with three-dimensional (3D) structure.[68] The top-view TEM image shows a uniform packing (Figure 3b). The structure consists of vertically arranged NCNTs which are sandwiched between the two N-doped graphene layers, forming a tight connection at the CNT−graphene interface. This allows both fast charge transport and efficient gas/electrolyte diffusion. The free-standing structure also results in a better physical contact among the cathode, collector, and electrolyte. As a result, the 3D NCNT/G-based Li−CO_2 battery owns high reversibility and low overpotential (Figure 3b). Meanwhile, the 3D structure has a high surface area and is rich in active sites for high-efficiency CO_2 reduction and evolution reactions. This cathode catalyst also shows a robust mechanical performance as well as high electrical conductivity, owing to the strong connection between NCNT and double-deck graphene sheets. All these characteristics pave the way for designing an efficient, free-standing, and binder-free cathode.

To better understand the ways in which theperformance of electrocatalysts can be optimized, a knowledge of the reaction mechanisms in place is essential. The possible reaction pathways of a reversible Li−CO_2 battery are discussed below.[69] During the discharge, Li^+ ions arising from the anode react with CO_2 at the cathode to form the discharge products (e.g., Li_2CO_3 and C) and produce electrical energy. C and CO are the common reduction products of CO_2 in the metal−CO_2 batteries, as shown in net reactions in eqs 1 and 2, with the later sharing a similar formation pathway of CO from CO_2 electrolysis.

$$4Li + 3CO_2 \Leftrightarrow 2Li_2CO_3 + C \quad (1)$$

$$2Li + 2CO_2 \Leftrightarrow Li_2CO_3 + CO \quad (2)$$

Elucidating the mechanisms for the formation of discharge products is beneficial for designing electrocatalysts. The detailed mechanism for Li_2CO_3 formation is shown in eqs 3−6. The initial step consists of a one-electron transfer to CO_2 to form the $C_2O_4^{2-}$ intermediate (eq 3). This intermediate can then decay through disproportionation into CO_2 and CO_2^{2-}, which may ultimately promote the formation of CO_3^{2-}. Thus, formation and nucleation of Li_2CO_3 follows as in eq 6.

$$2CO_2 + 2e^- \rightarrow C_2O_4^{2-} \quad (3)$$

$$C_2O_4^{2-} \rightarrow CO_2 + CO_2^{2-} \quad (4)$$

$$CO_2^{2-} + C_2O_4^{2-} \rightarrow C + 2CO_3^{2-} \quad (5)$$

$$2Li^+ + CO_3^{2-} \rightarrow Li_2CO_3 \quad (6)$$

Heterogeneous electrocatalysts play an essential role in providing a catalytic site to then promote the decomposition of the discharge product. However, several aspects of this process still remain unexplored. We illustrate a possible decomposition mechanism of Li_2CO_3 in eqs 6−8.[70] The unimolecular decay of Li_2CO_3 is followed by CO_2 and O_2 evolution at a higher voltage (3.8 V), as in eq 7. By contrast, CO_2 is the only gaseous product formed at lower voltage (2.8 V) by interaction of the starting Li_2CO_3 with C species (eq 8). A third possible pathway includes decomposition of the electrocatalyst surface to form superoxide species which are then likely to undergo further reaction to form an array of different products (eq 9).

https://doi.org/10.1021/acsenergylett.2c02445
ACS Energy Lett. 2023, 8, 1818−1838

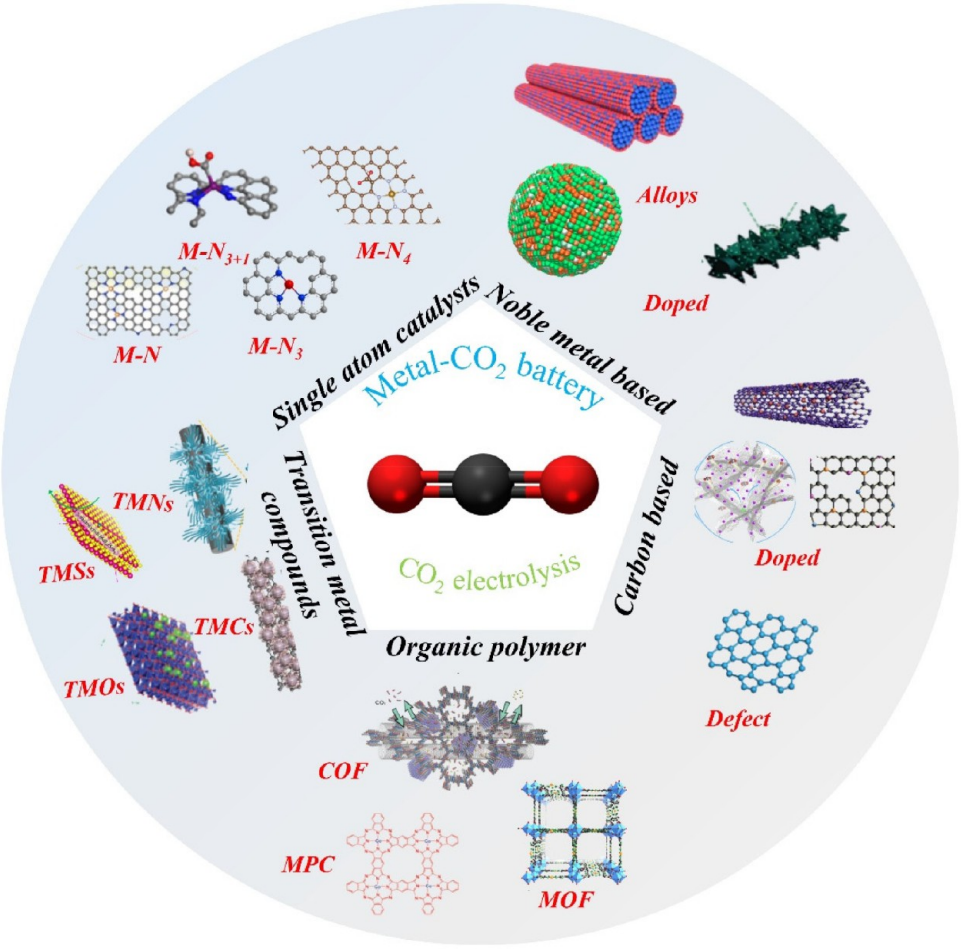

Figure 1. Overview of different types of electrocatalysts for metal−CO_2 batteries and CO_2 electrolysis. The inserted graphics are adapted with permission from ref 67, American Chemical Society 2021; ref 71, Wiley 2019; ref 73, Elsevier 2020; ref 80, Wiley 2022; ref 84, American Chemical Society 2019; ref 100, Wiley 2017; ref 102, American Chemical Society 2022; ref 103, Wiley 2019; ref 110, Wiley 2021; ref 114, Wiley 2021; ref 117, Wiley 2022; ref 119, American Chemical Society 2022; ref 109, Wiley 2021; ref 111, Wiley 2020; ref 113, Wiley 2022; ref 131, Wiley 2019; ref 133, The Royal Society of Chemistry 2018; ref 134, Wiley 2019.

Table 1. Different Types of Electrocatalysts for Metal−CO_2 Batteries and Their Electrocatalytic Performance

catalyst	discharging capacity (current density)	overpotential (current density)	cycle number (current density)	ref
CA-NG/RGO		2.13 V (1.2 A g^{-1})	170 cycles (500 mA g^{-1})	67
TDG	69000 mAh g^{-1} (0.5 A g^{-1})	1.87 V (2.0 A g^{-1})	600 cycles (1.0 A g^{-1})	72
Ru/NS-G	12448 mA h g^{-1} (100 mA g^{-1})	1.40 V (100 mA g^{-1})	100 cycles (100 mA g^{-1})	73
BCNT	23328 mAh g^{-1} (1000 mA g^{-1})	1.96 V (1000 mA g^{-1})	360 cycles (1000 mA g^{-1})	71
NCNT/G	17534.1 mAh g^{-1} (100 mA g^{-1})	1.13 V (100 mA g^{-1})	180 cycles (100 mA g^{-1})	68
RuP_2−NPCF	11951 mAh g^{-1} (100 mA g^{-1})	1.77 V (100 mA g^{-1})	200 cycles (1000 mA g^{-1})	86
CNT/RuO_2	2187 mAh g^{-1} (50 mA g^{-1})	1.40 V (50 mA g^{-1})	55 cycles (50 mA g^{-1})	84
Ru−Co_3O_4/CC	31000 mAh g^{-1} (100 mA g^{-1})	1.05 V (200 mA g^{-1})	251 cycles (200 mA g^{-1})	114
$Ru(bpy)_3Cl_2$	22119 mAh g^{-1} (200 mA g^{-1})	1.79 V (300 mA g^{-1})	60 cycles (300 mA g^{-1})	116
Ir−Te	13274 mAh g^{-1} (200 mA g^{-1})	1.48 V (200 mA g^{-1})	350 cycles (200 mA g^{-1})	85
ReS_2	1800 μAh cm^{-2} (40 μA cm^{-2})	0.66 V (20 μA cm^{-2})		95
Co-MnO_2	8160 mAh g^{-1} (100 mA g^{-1})	0.73 V (100 mA g^{-1})	500 cycles (100 mA g^{-1})	103
MoN@CC	6542 μAh cm^{-2} (20 μA cm^{-2})	0.36 V (20 μA cm^{-2})	86 cycles (20 μA cm^{-2})	117
Mo_2C		0.94 V (500 μA cm^{-2})		100
N-carbons	10500 mAh g^{-1} (300 mA g^{-1})		80 cycles (1000 mA g^{-1})	
MWCNT	60000 mAh g^{-1} (1000 mA g^{-1})	1.5 V (1000 mA g^{-1})	200 cycles (1000 mA g^{-1})	74
Pd In		0.161 V (0.1 mA cm^{-2})		28
Au		0.11 V (0.1 mA cm^{-2})		118
Mn-MOF	18022 mAh g^{-1} (50 mA g^{-1})	1.31 V (200 mA g^{-1})	50 cycles (200 mA g^{-1})	131
hydrazone/hydrazide COF	27348 mAh g^{-1} (200 mA g^{-1})	1.24 V (200 mA g^{-1})	200 cycles (1000 mA g^{-1})	132

https://doi.org/10.1021/acsenergylett.2c02445
ACS Energy Lett. 2023, 8, 1818−1838

Table 2. Different Electrocatalysts for Electrochemical CO_2 Reduction

catalyst	electrolyte	FE% (voltage)	main product	current density (mA cm^{-2})	ref
K-defect-C	0.1 M $KHCO_3$	99 (−0.45 V vs RHE)	CO	9.8	80
Ag−Cu	0.1 M $KHCO_3$	40 (−0.11 V vs RHE)	C_2H_4	750	89
Pd_2	0.5 M $KHCO_3$	98.2 (−0.85 V vs RHE)	CO	6.76	106
Ag_1/MnO_2	0.5 M $KHCO_3$	95.7 (−0.85 V vs RHE)	CO	3.4	116
Phen-Cu	0.1 M $KHCO_3$	83 (−0.5 V vs RHE)	CO/HCOOH	2	103
Ni−N_3−C	0.5 M $KHCO_3$	95.6 (−0.65 V vs RHE)		6.64	109
Zn/NC	0.5 M $KHCO_3$	98 (−0.6 V vs RHE)		50	113
Zn-MOF	0.1 M $KHCO_3$	90.57 (−1.1 V vs RHE)		4	126

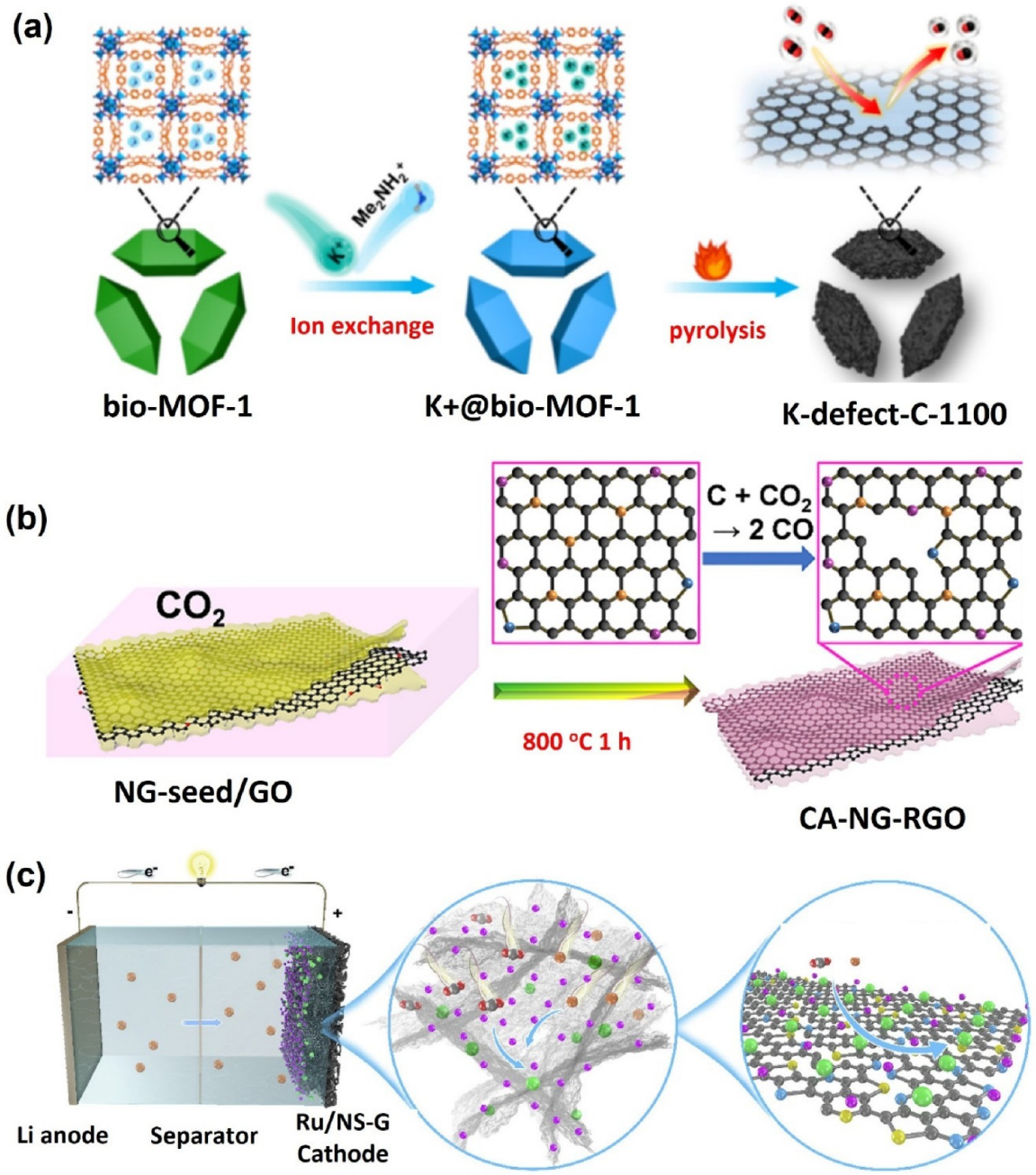

Figure 2. (a) Illustration for the fabrication of K-defect-C-1100 via the K^+-assisted strategy. The introduction of K^+ to give K^+@bio-MOF-1 by ion exchange is crucial in the first step, prior to the pyrolysis. Adapted with permission from ref 80. Copyright 2022, Wiley-VCH. (b) Schematics of the synthesis of CA-NG/RG. Adapted with permission from ref 67. Copyright 2021, American Chemical Society. (c) Schematic illustration of the processes in Li−CO_2 battery with Ru/NS-G cathode, and the specific roles of the Ru nanoparticles and the heteroatoms. Adapted with permission from ref 73. Copyright 2020, Elsevier.

https://doi.org/10.1021/acsenergylett.2c02445
ACS Energy Lett. 2023, 8, 1818−1838

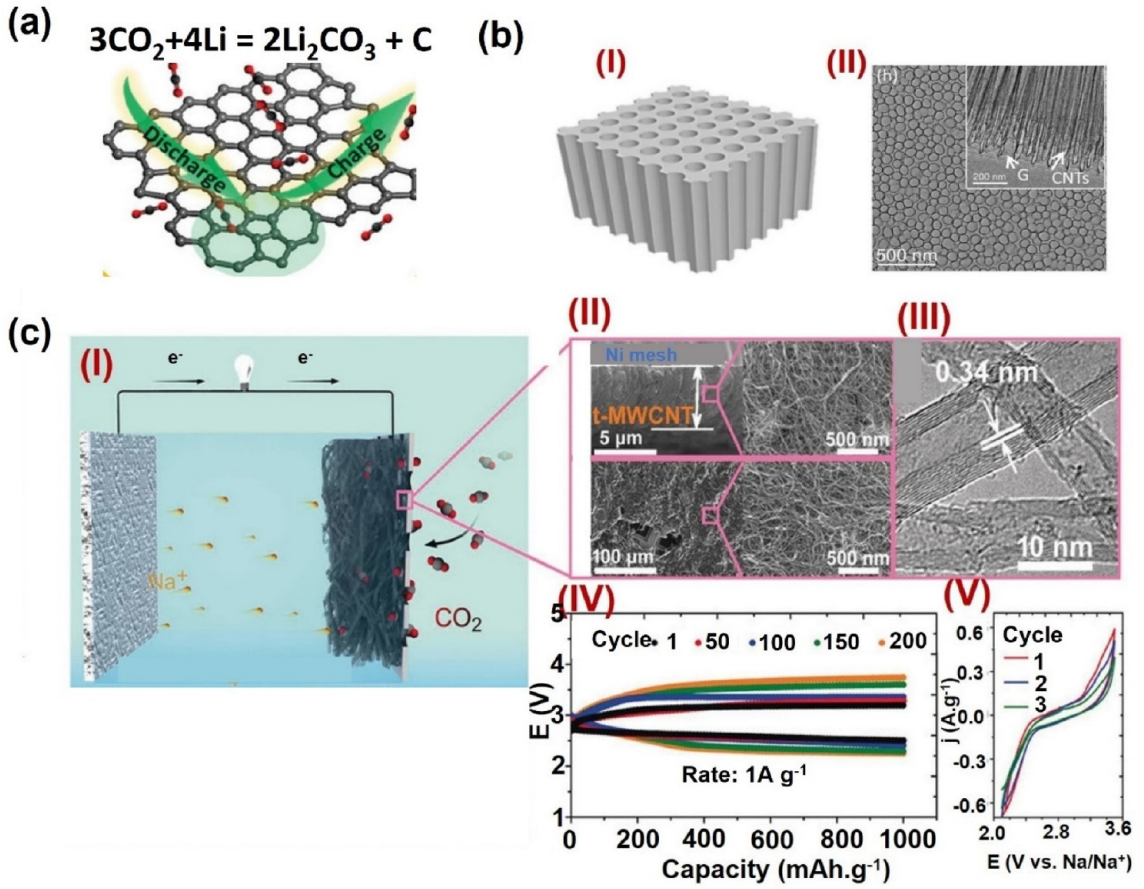

Figure 3. (a) Schematic illustration of a Li−CO_2 battery assembly. Adapted with permission from ref 72. Copyright 2021, Wiley-VCH. (b) (I) Schematic illustration of 3D NCNT/G and (II) top view and cross-sectional (inset) TEM images of 3D NCNT/G. Adapted with permission from ref 68. Copyright 2020, American Chemical Society. (c) The structure and rechargeability of room-temperature Na−CO_2 batteries. (I) Structure of Na−CO_2 batteries with metal Na foil anode, ether-based electrolyte, and t-MWCNT cathode. (II) SEM images of cathode from top and side views. (III) HRTEM image of t-MWCNT. (IV) Discharge and charge profiles of Na−CO_2 batteries at 1 A g^{-1}. (V) CV curves of Na−CO_2 batteries with scan rate of 0.1 mVs^{-1}. Adapted with permission from ref 74. Copyright 2016, Wiley-VCH.

$$2Li_2CO_3 \rightarrow 4Li^+ + CO_2 + O_2 + 4e^- \quad (7)$$

$$2Li_2CO_3 + C \rightarrow 4Li^+ + 3CO_2 + 4e^- \quad (8)$$

$$2Li_2CO_3 + \text{electrocatalyst} \rightarrow CO_2 + 2Li^+ + O_2^{\cdot-} \rightarrow \text{unknown product(s)} \quad (9)$$

Among others, the current density is a key factor for reaction kinetics and has a huge impact on determining which decomposition pathway is most active for the discharge product in the Li−CO_2 battery. Careful evaluation of these factors will lead to a better understanding of the reaction principles and ultimately assist the design of more efficient electrocatalysts.[49]

Akin to NCNT/G 3D structure, the bamboo-like N-CNT (B-NCNT) demonstrated by Li et al. also follows the strategy of offering rich active sites to improve cycle performance and decrease overpotential for the Li−CO_2 battery.[71] CNTs are typically straight cylinders, but the presence of pentagonal pyridine N and hexagonal pyridine N forms a positive curvature, which facilitates the closure of the nanotubes and enables them to transform into a bamboo form with significant periodic nodes. The abundance of defects and active sites, followed by the interconnected conductive network, can promote both the reduction and evolution of CO_2 reactions. The doped N atoms act as the main active sites and enable stable electrocatalytic performance. The experimental results are consistent with the theoretical predictions. The Li−CO_2 battery fabricated with the B-NCNT cathode shows an outstanding discharge capacity of 23328 mAh/g and low overpotential of 1.96 V at a high current density of 1000 mA/g. This demonstrates the advantage of the B-NCNT cathode, which may aid in achieving high capacity with relatively high efficiency at high current density. In addition, Li et al. used a metal substrate Ti with a high degree of flexibility and a forest of carbon nanotubes grown uniformly in situ to ensure the flexibility of the cathode under different bending angles (0°, 30°, 45°, 60°). In conclusion, the performance improvement brought by the bamboo-like structure was successfully proved. The work provides a guideline for a metal-free cathode to be employed in wearable electronics.

Constructing a 3D structure and introducing doping atoms both become promising strategies to enhance the electrocatalytic performance of carbon-based electrocatalysts.

https://doi.org/10.1021/acsenergylett.2c02445
ACS Energy Lett. 2023, 8, 1818−1838

To further study the influence of defects in carbon-based electrocatalysts, graphene with rich topological defects (TDG) has been used as cathode electrocatalyst to assemble Li−CO_2 batteries.[72] The defects are introduced through removing N dopants, as shown in Figure 3a. The Li−CO_2 battery with the TDG cathode shows an excellent Coulombic efficiency (90.80%) and an impressive low voltage gap (1.12 V at 100 mA/g). The improved performance can be attributed to the abundant active sites provided by TDG which can enhance the formation of Li_2CO_3. The interconnected graphene nanosheets (NSs) with large surface area can improve the electron transport and ion/gas diffusion. At the same time, it also can increase the intake of Li_2CO_3 to achieve a high level of capacity. This work shows the advantage of introducing the defects for designing a superior carbon-based catalyst for a metal−CO_2 battery which can facilitate Li_2CO_3 decomposition and CO_2 reduction.

Hence, constructing a 3D structure and simultaneously introducing doping atoms become promising strategies to enhance the electrocatalytic performance of carbon-based electrocatalysts. Qiao and co-workers designed and developed a 3D structure of N,S-codoped graphene with ultrafine Ru nanoparticles (Ru/NS-G) by combining these two strategies.[73] An illustration of a Li−CO_2 battery with the cathode of Ru/NS-G is shown in Figure 2c. The powerful synergistic effect between the N and S codopants as well as the presence of the bifunctional Ru catalyst can provide rich defect structure and active sites for the adsorption of CO_2 and the decomposition of the discharge product. During the process of charging and discharging, three different types of N-sites in the cathode catalyst play different roles: pyrrolic-N and pyridinic-N are favorable for adsorption of Li^+ and CO_2, while the graphitic-N sites can effectively improve the conductivity of the cathode. In addition, the insertion of S atoms into the sp^2-hybridized carbon skeleton can further improve electrocatalytic activity.

Chen et al. reported a rechargeable Na−CO_2 battery with the cathode composed of a multiwall carbon nanotube (t-MWCNT) material treated by tetraethylene glycol dimethyl ether (TEGDME) electrolyte.[74] The cathode exhibits a 3D, porous cross-linking architecture, as shown in Figure 3c. The particular structure of the conductive network can play an important role in accommodating a high amount of discharge product, here Na_2CO_3. In this way, the highly porous structure of the cathode appears to prevent blockage of the gas channel and thus improves the cycle performance. It was demonstrated that the constructed battery could run 200 cycles under a high current density (1 A/g) (Figure 3c). This work demonstrates that the carbon-based cathode electrocatalysts can provide a high surface area for a Na−CO_2 battery to enhance cycle performance and decrease overpotential. Similar to the reaction of the reversible Li−CO_2 battery, the reversible Na−CO_2 battery follows an analogous mechanism: $4Na + 3CO_2 \Leftrightarrow 2Na_2CO_3 + C$. In addition, prior treatment of the cathode with the electrolyte is beneficial for promoting the reaction kinetics occurring at the surface and interface of the material.

Carbon-based catalysts doped by nonmetal atoms shows a high electrocatalytic performance for Li−CO_2 batteries. It is still necessary to develop carbon-based electrocatalysts to meet the requirements of higher conductivity, larger surface area, and better binding affinity with CO_2. Therefore, Hu et al. employed N-doped nanocarbon for a solid-state Na−CO_2 battery for the first time.[75] The cathode catalyst comes from the zeolitic imidazolate frameworks (ZIFs) and exhibit excellent electrocatalytic activity, good affinity with CO_2 molecules, and impressive conductivity. The authors reported a systemic study on the effects of doping atoms, CO_2 adsorption, and electrical conductivity on the electrochemical performance of the Na−CO_2 battery. In the presence of such a catalyst, the discharge product (Na_2CO_3) can easily form a sheet structure, which can be decomposed to CO_2 during the charging process. According to the results of density functional theory, the C=O bonds of absorbed CO_2 molecules have uneven length that match with C−O bonds in Na_2CO_3. This study provides more insight into the behavior of adsorbed CO_2 molecules on the N-doped nanocarbon surfaces. The experimental results also show that the Na−CO_2 battery using N-doped nanocarbon cathode has a lower overpotential (1.5 V) and a higher discharge performance (10500 mAh/g).

Furthermore, constructing heteroatom-doped carbon also became a feasible way to improve the performance of carbon-based electrocatalysts for CO_2 electrolysis.[76,77] Li et al. reported on the N-doped porous carbon obtained from coal (CNPC), which shows a synergistic effect of unique porous structure and high amounts of N defects.[78] The results show that CNPC exhibits a high-efficiency conversion from CO_2 to CO (92%). The work provides a low-cost and facile method to synthesize metal-free electrocatalysts for CO_2 electrolysis. Besides, one of the major challenges for CO_2ER is to improve conversion efficiency. Other heteroatom-doped carbon-based electrocatalysts also provide a promising way to solve this problem. For example, the fluorine-doped cage-like porous carbon (F-CPC) is proposed to achieve superior FE (88.3%) at a higher current density (37.5 $mA{\cdot}cm^{-2}$).[79] The impressive performance is attributed to the improved structural properties, which feature a large amount of moderate mesopores and rich micropores.

However, although doping appears to be a promising strategy to promote activation in electrocatalysts, the intrinsic properties of defects in doped carbon-based materials are often disregarded. In fact, carbon atoms at the edge of defects in different microenvironments are often rich in dangling bonds; thus, they become greatly activated due to the uneven charge distribution. Therefore, it is worth synthesizing defective but dopant-free carbon catalysts to study the influence of carbon defects without the interference of other factors.

Based on this idea, Ling et al. developed a K^+-assisted strategy to make carbon defects without N dopants, via the design of an anionic metal−organic framework (MOF).[80] MOFs play a very important role in constructing porous carbon with the advantages of component and structural regulation. The synthesis procedure for this material is shown in Figure 2a. First, the authors selected an anionic MOF with the Me_2NH^{2+} (dimethylammonium cations) in a 1D channel for preparation of ion exchange, wherein the Me_2NH^{2+} can be replaced with K^+. After exchanging ions, the resulting K^+@bio-MOF-1 was pyrolyzed to successfully obtain a carbon skeleton rich in 12-vacancy-type defects (K-defect-C-1100), wherein 12 neighboring carbon atoms are missing. K^+ activation was found to induce larger vacancies/holes and in larger numbers. Plus, a higher density of carbon sites with dangling bonds was prepared in this material. Electron-rich carbon sites enhance adsorption of the mildly electrophilic CO_2 molecules, thus further favoring the ensuing CO_2ER reaction when compared to more localized ring defects present in other materials. As a result, the prepared materials display excellent CO Faradaic efficiency and higher electrocatalytic activity, cf. more established N-doped carbon catalysts. This implies that the K-defect-C-1100 shows a high selectivity for forming CO. The mechanism of CO formation by

https://doi.org/10.1021/acsenergylett.2c02445
ACS Energy Lett. 2023, 8, 1818−1838

CO_2ER is shown in eqs 10−12, wherein the "*" represents the active sites (i.e., adsorption site). The heterogeneous electrocatalysts play an important role in providing active sites, which have the ability to bind to reactants, intermediates, and products, thus stabilizing them. From this, it can be assumed that K-defect-C-1100 favors the formation of the COOH* (eqs 10 and 11) species, which is the crucial intermediate ultimately leading to the formation of CO. If the interactions between the CO and the active site is labile, the product will then desorb from the surface, as in eq 12.

$$CO_2(g) + {}^* + H^+(aq) + e^- \rightarrow {}^*COOH \quad (10)$$

$$^*COOH + H^+(aq) + e^- \rightarrow H_2O(l) + {}^*CO \quad (11)$$

$$^*CO \rightarrow CO(g) + {}^* \quad (12)$$

In conclusion, carbon-based electrocatalysts are still the most feasible electrocatalysts to be applied in both metal−CO_2 batteries and CO_2 electrolysis.[81] In the metal−CO_2 batteries, the carbon electrocatalysts can provide a high surface area to boost the movement of CO_2/electrons and accommodate the discharge product(s). Therefore, they become important candidates as electrocatalysts for metal−CO_2 batteries with a metal-free electrode. Carbon-based electrocatalysts also play an essential role in the field of CO_2 electrolysis, and they are particularly beneficial for very similar reasons (i.e., excellent conductivity and high surface area). More importantly, the improved strategies for carbon-based electrocatalysts can enhance electrochemical performance of both metal−CO_2 batteries and CO_2 electrolysis. For example, introducing defects into the carbon skeleton can greatly boost the electron transfer rate to benefit these two applications. In addition, carbon-based electrocatalysts also can act as the support for other electrocatalysts to provide abundant active sites. In this way, the carbon-based electrocatalysts pave the way for next-generation electrocatalysts for metal−CO_2 batteries and CO_2 electrolysis.[82,83]

NOBLE METAL-BASED ELECTROCATALYSTS

Noble metal-based electrocatalysts have also become promising materials to improve the kinetics of CO_2ER. Designing well-fined structures for noble metal-based electrocatalysts has become an emerging strategy to further boost electrocatalytic performance.[84] For instance, the superassembled atomic Ir dispersed on the amorphous surface layer of Te nanowires (Ir−Te NWs) is precisely designed to ensure stable reaction kinetics for both charging and discharging process in Li−CO_2 batteries.[85] This special architecture provides a guideline for the design of novel electrocatalysts and benefits from exposing a large number of Ir active sites which can effectively adsorb/desorb adsorbates. Moreover, the Te substrate favors the adsorption of Li^+ and CO_2 with high efficiency. Thus, the substrate can effectively facilitate CO_2ER on Ir active sites and the formation of $Li_2C_2O_4$ (instead of Li_2CO_3) to achieve lower charge potential.

The derivatives of noble metal electrocatalysts have been explored for the development of metal−CO_2 batteries, especially Li−CO_2 batteries. For example, the highly disperse RuP_2 nanoparticles (NPs) supported by N- and P-doped carbon films (RuP_2−NPCF) facilitate the conversion between CO_2 and Li_2CO_3.[86] The fabricated porous NPCF can enhance the electrode conductivity and provide more active sites for RuP_2, thus boosting the decomposition of the discharge product. Based on the same idea, the RuO_2@CNT formed by RuO_2 decorated on CNT owns a better cycle performance and lower charging potential compared with pure CNT.[84] These works show the ability of derivatives of noble metal electrocatalysts to decompose discharge product(s) and lower the overpotential of metal−CO_2 battery.

Noble metal-based materials also play a vital role in CO_2 electrolysis and offer a pathway for effectively converting this greenhouse gas to useful carbon products.[87,88] Until now, considerable work has focused on elucidating the effects of size, shape, chemical state, and particle boundaries on electrocatalytic performance. Recently, it has been found that the synthesis of bimetallic electrocatalysts can greatly improve electrocatalytic efficiency. Judicious preparation of bimetallic catalysts can aid in adjusting the binding strength or binding configuration of the surface intermediates, thus allowing high selectivity for specific products and improved catalytic activity. For example, the Ag−Cu NPs shows a higher electrocatalytic performance for CO_2ER to ethylene (C_2H_4) in comparison with Cu NPs of similar size and shape.[89] More importantly, this work reveals that sequential catalysis and electronic effects are the main factors for increased selectivity for C_2H_4 in the bimetallic catalyst. Thus, the work provides valid insights into the design of high-efficiency noble metal electrocatalysts for the CO_2 reduction reaction. The net reaction to form C_2H_4 upon CO_2ER is shown in eq 13:

$$CO_2 + 12H^+ + 12e^- \rightarrow C_2H_4 + 4H_2O \quad (13)$$

The role of supporting materials in electrocatalysis is also fundamental. Noble metals supported by different materials (oxides, carbons, etc.) have also been extensively studied as a means to improve the stability and activity of noble metal-based electrocatalysts.[90−93] First, the use of supporting materials is beneficial to increase the surface area of noble metals. Therefore, investigating the interaction between noble metals and supporting materials is helpful to design noble metal-based electrocatalysts with high electrocatalytic activity, long-term stability, and cost-effectiveness. In this context, the Au-CeO_x electrocatalyst is a representative example of a noble metal supported by a transition metal oxide.[94] The interface between Au and CeO_x plays an important role in improving CO_2 adsorption and offering active sites for CO_2 conversion. More importantly, the key intermediate product *COOH is further stabilized by the synergistic effect between Au and CeO_x. As such, this work shows that superior electrochemical performance (FE: 89.1% at −0.89 V) can be obtained because of the unique Au−CeO_x interface.

In conclusion, noble metal-based electrocatalysts are promising electrocatalysts to be commercialized because of their excellent electrocatalytic performance.[86,95] They can provide good cycle stability and charge/discharge ability in metal−CO_2 batteries. They are also good candidates to boost the reaction kinetics of CO_2 electrolysis. Therefore, noble metal-based electrocatalysts represent a class of electrocatalysts which can be employed for the development of metal−CO_2 batteries and CO_2 electrolysis technologies.[96−98] However, the well-known downside of such catalysts is their high cost, which has long been a concern especially for large-scale applications. Thus, much of the current research is focused on finding low-cost and abundant alternatives to noble metals with comparable electrocatalytic performance, in the attempt to reduce the burden of the high cost of raw materials in manufacturing.

https://doi.org/10.1021/acsenergylett.2c02445
ACS Energy Lett. 2023, 8, 1818−1838

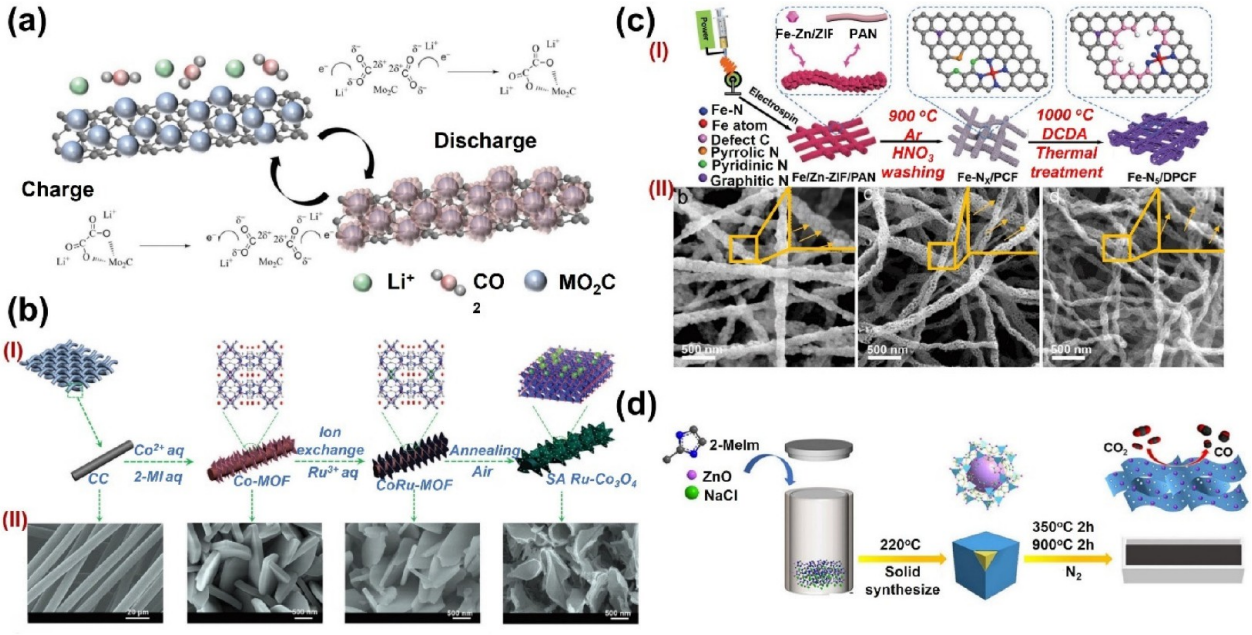

Figure 4. (a) Schematic illustration of reactions during discharge and charge of Mo_2C/CNT in the Li−CO_2 battery. CO_2 is reduced at the Mo_2C/CNT electrode surface on discharge, forming $Li_2C_2O_4$, and then this intermediate product is stabilized by Mo_2C, forming an amorphous discharge product that can be easily decomposed on charge. Adapted with permission from ref 100. Copyright 2017, Wiley-VCH. (b) Structure characterization of SA Ru−Co_3O_4/CC. (I) Illustration of the synthesis process of SA Ru−Co_3O_4/CC. (II) SEM images of CC, Co-MOF/CC, CoRu-MOF/CC, and SA Ru−Co_3O_4/CC (from left to right). Adapted with permission from ref 114. Copyright 2021, Wiley-VCH. (c) (I) Schematic diagram of the preparation procedure of Fe−N_5/DPCF. (II) SEM images of Fe/Zn-ZIFs/PAN, Fe−N_x/PCF and Fe−N_5/DPCF (from left to right). Adapted with permission from ref 112. Copyright 2022, Wiley-VCH. (d) Diagram for the synthesis of Zn/NC NSs. Adapted with permission from ref 113. Copyright 2022, Wiley-VCH.

TRANSITION METAL COMPOUND-BASED ELECTROCATALYSTS

Transition metal-based electrocatalysts (carbides, sulfides, nitrides, and phosphates) play an essential role in a variety of electrocatalytic reactions.[99] For instance, molybdenum carbide (Mo_2C) has attracted much attention due to its excellent electrocatalytic performance as one kind of carbide. Mo_2C is widely used in a variety of electrocatalytic reactions, such as water gas shift reaction and hydrogen evolution reaction, but it has rarely been used in the field of metal−CO_2 batteries. Hou et al. reported Mo_2C/CNT acts as a good cathode electrocatalyst to improve the rechargeable ability of Li−CO_2 batteries.[100] CNTs act as conductive substrates to provide high surface area for supporting evenly dispersed Mo_2C NPs. The cathode with Mo_2C showed a better electrical efficiency and reversibility because of its partially oxidized surface. By introducing the carbon support, Mo_2C owns higher activity due to the ensuing change in its electronic properties and increased reactivity of adsorbates (Figure 4a). According to the results of XPS, the content of Mo^{2+}, Mo^{3+}, and Mo^{5+} decreases sharply after discharge, but the content of Mo^{6+} increases, which indicates that the Mo ion changes from a lower valence state to a higher valence state during this process. The authors also shed light on the mechanism of a Li−CO_2 battery with the cathode catalyst of Mo_2C/CNT. The proposed reaction mechanism is shown in eqs 14 and 15:

$$2CO_2 + 2e^- \rightarrow C_2O_4^{2-} \quad (14)$$

$$C_2O_4^{2-} + 2Li^+ + Mo_2C \rightarrow LiC_2O_4{-}Mo_2C \quad (15)$$

Metal−oxygen coupling between Mo and O via the transfer of coordinative electrons can stabilize the otherwise unstable $C_2O_4^{2-}$ to form amorphous $Li_2C_2O_4$−Mo_2C, as opposed to Li_2CO_3. Therefore, the Li^+ and CO_2 will be easily released by cleaving the Mo−O bond, thus reducing the overpotential (Figure 4).

Wang's group used density functional theory (DFT) computations and confirmed that $Li_2C_2O_4$ is the main discharge product when Mo_2C acts as a cathode catalyst.[101] They further studied the commonly exposed crystal structure of Mo_2C, α-Mo_2C(001), β-Mo_2C(001), as well as β-Mo_2C(101), revealing that (001) and (101) catalyst surfaces of β-Mo_2C have the lowest ΔG for the nucleation of the discharge product and the lowest overpotential, respectively.

Akin to Mo_2C with high electrocatalytic activity, molybdenum disulfide (MoS_2) also has been widely utilized as a promising catalyst.[102] In comparison with the inactive basal plane sites, the active edge sites of MoS_2 (unsaturated S atoms) play an important role in catalysis. If present in large excess, the in-plane S atoms within the Mo_2S nanosheet become redundant or unutilized and may even limit the activity of Mo_2S. It is inferred that improving the electrocatalytic performance relies on fully utilizing the available S atoms during the catalytic process. Herein, MoS_2/SnS_2 superthin nanosheets were synthesized to act as a cathode for Na−CO_2 batteries. By introducing SnS_2, more in-plane S vacancies are induced on the MoS_2/SnS_2 basal site. This is found to facilitate CO_2 adsorption. In addition, SnS_2 incorporation can enhance the Na^+ charge-transfer mobility, resulting in better cycle performance and lower overpotential compared to the pure MoS_2 electrocatalyst.

ReS_2 is another type of disulfide electrocatalysts applied for metal−CO_2 batteries.[95] The ReS_2 takes advantage of the

https://doi.org/10.1021/acsenergylett.2c02445
ACS Energy Lett. 2023, 8, 1818−1838

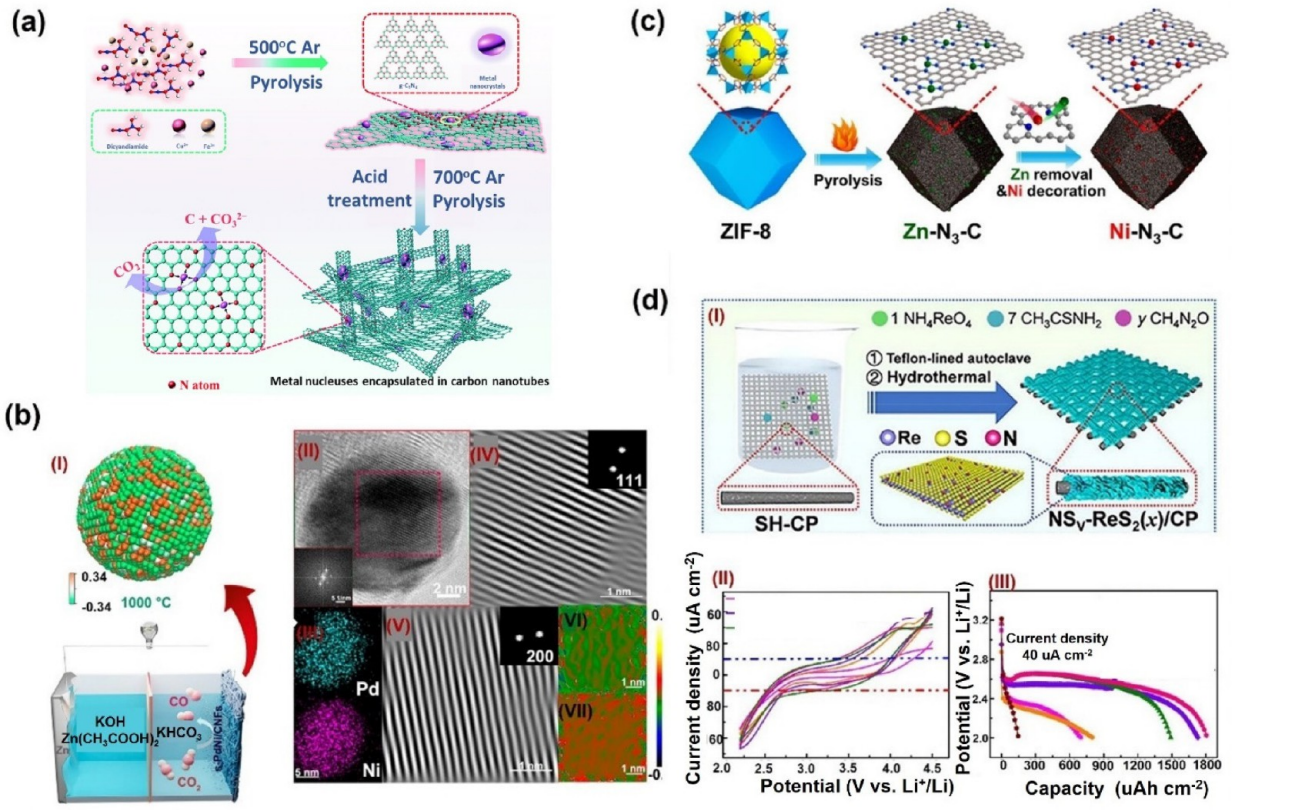

Figure 5. (a) Schematic illustration of preparation procedures for Fe−Cu−N−C and the possible microstructure of the Fe−Cu−N−C catalyst. Adapted with permission from ref 108. Copyright 2021, The Royal Society of Chemistry. (b) (I) Model for the aqueous rechargeable Zn−CO_2 battery equipped with s-PdNi/CNFs-1000 as the cathode. (II) AC-TEM image of s-PdNi-800 NPs. (III) EDS mapping images of s-PdNi-800 NPs. IFFT patterns of the (IV) (111) and (V) (200) planes of s-PdNi-800 NPs. Corresponding strain distributions of e_{xx} and e_{xy} on s-PdNi-800 were in line with the (VI) (111) and (VII) (200) planes. Adapted with permission from ref 119. Copyright 2022, American Chemical Society. (c) Fabrication of low-coordination single-atom Ni electrocatalysts via a PSMS strategy. Adapted with permission from ref 109. Copyright 2021, Wiley-VCH. (d) (I) Schematic of the synthesis process of NSV-ReS_2(x)/CP. (II) CV curves at a scanning rate of 0.2 mV s^{-1} and (III) fully discharging curves at 40 μA cm^{-2} for the five cells (pink line, NS_V- ReS_2; yellow line, NS_V-ReS_2(8/7)/CP; purple line, NS_V-ReS_2(3)/CP; red line, NS_V-ReS_2(5)/CP; green line, NS_V-ReS_2(7)/CP; brown line, NS_V-ReS_2(7)/CP). Adapted with permission from ref 95. Copyright 2022, American Chemical Society.

synergistic effect between nucleophilic N dopant and electrophilic S vacancy (Figure 5d, part I). This particular electronic structure affects the interaction between the Li atoms and C/O atoms, thus favoring the adsorption of crucial reaction intermediates. Therefore, the Li−CO_2 battery with NSV-ReS_2(5)/CP shows excellent cycle performance and discharging ability (Figure 5d, parts I and II).

An additional cathode catalyst, Co-doped MnO_2 nanowires (NWs), was proposed by Peng and co-workers,[103] who worked on directly optimizing the electrode structure. The authors found that the introduction of cobalt can effectively improve the electrode conductivity by lowering the bandgap of MnO_2. Furthermore, it increases the porosity of the electrode with pores of multiple sizes, thus easing the diffusion of electrolyte and the movement of CO_2. The Li−CO_2 battery with Co-interstitial MnO_2 NWs owns an ultralow overpotential (0.73 V) and stable cycle performance (over 500 cycles at the current density of 100 mA/g), which provide novel avenues for designing high-efficiency nonnoble metal-based electrocatalysts.

Morphology engineering for nanomaterials can adjust surface and interfacial properties to increase the surface area and improve reaction kinetics. This inspired researchers to design and develop different methods to synthesize multidimensional nanomaterials. However, the unfavorable factors, such as costly equipment, intricate experimental procedure, and environmentally unfriendly reactants are the main drawbacks for the development of such synthetic processes. Therefore, Xu et al. used the self-assembly strategy to control the growth of $CuCo_2O_4$ (CCO) materials for Na−CO_2 batteries (Figure 6d).[104] $NH_3{\cdot}H_2O$ plays a role in modulating pH to induce oriented growth of the precursors (p-CCO). At low pH (pH 2), accumulation of p-CCO is the main growth behavior, because $NH_3{\cdot}H_2O$ is difficult to coordinate with p-CCO. With the increase of pH, NH_3 molecules are more likely to coordinate with copper ions, and the growth rate of p-CCO in the axial direction is accelerated. Therefore, the morphology of the material is gradually transformed from spherical to rod-like. When pH is between 6 and 7, directional growth becomes the dominant factor; thus, the material finally grows into a one-dimensional morphology. They also found that the highly conductive polypyrrole (PPy) shell creates conductive channels for the active material to improve electrical conductivity, speeds up electron transfer, and reduces electrolyte corrosion during long-term operation. Finally, the 1D rod-like $CuCo_2O_4$/PPy (CCO/ppy) exhibiting rich oxygen vacancies and active sites demonstrates an impressive potential gap (0.6 V, over 600 cycles) and excellent discharge capacity (31.3 mAh cm^{-2}).

https://doi.org/10.1021/acsenergylett.2c02445
ACS Energy Lett. 2023, 8, 1818−1838

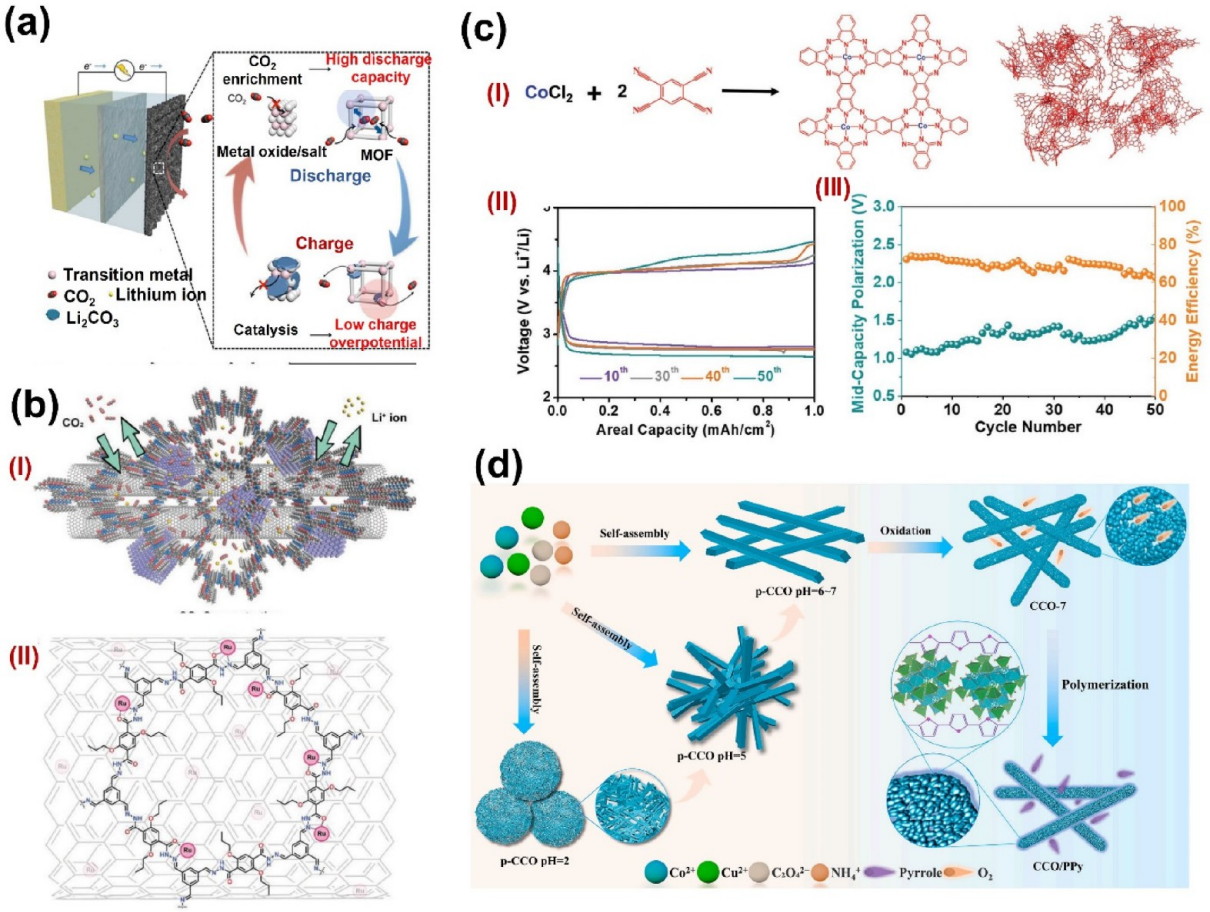

Figure 6. (a) Scheme of the advantages of a Li−CO_2 battery equipped with a MOF-based CO_2 electrode. Adapted with permission from ref 133. Copyright 2018, The Royal Society of Chemistry. (b) Synthesis of highly crystalline Tf−DHzOPr COF interfaced with Ru@CNT via hydrazide−metal coordination. Adapted with permission from ref 134. Copyright 2019, Wiley-VCH. (c) (I) Schematic synthetic process of 2D CoPPc. Electrochemical performance of Li−CO_2 batteries using CoPPc as the cathode catalyst. (II) Charge and discharge voltage profiles at 0.05 mA cm^{-2} with a cutoff capacity of 1 mAh cm^{-2}. (III) Change of the midcapacity polarization and energy efficiency with the cycle number. Adapted with permission from ref 131. Copyright 2019, Wiley-VCH. (d) The growth mechanism and microstructure of 1D rod-like CCO/PPy. Adapted with permission from ref 104. Copyright 2022, Elsevier.

Similar to metal−CO_2 batteries, CO_2 electrolysis can also benefit from the advantages of transition metal compound-based electrocatalysts. The reduction process of CO_2 consists of several basic steps and is accompanied by the formation of various intermediates. The process is intrinsically complex, with an additional complication arising from the competition with the hydrogen evolution reaction. Therefore, designing and developing electrocatalysts with high electrocatalytic activity and excellent selectivity has become one of the hot issues in this field. Luckily, the transition metal compound-based electrocatalysts with diverse composition (oxides, sulfides, carbides, and nitrides) and various sizes (molecular level, nanostructure, and microstructure) provide a feasible way to tackle the current challenges. For example, the molecular 1,10-phenanthroline-Cu compound supported by mesostructured graphene can achieve a high activity and selectivity toward CO_2 reduction.[105] A possible pathway to form HCOOH is illustrated in eq 16:

$$CO_2 + 2H^+ + 2e^- \rightarrow HCOOH \quad (16)$$

The Cu^+ active site forms a trigonal bipyramidal structure with the neighboring N atoms and initiates the catalysis from the η^1-COO-like configuration. The phen-Cu can achieve a high electron density through voltage adjustment, which shows a strong ability to control the electron distribution of CO_2. These factors can facilitate CO_2 adsorption. In addition, the supported mesostructured graphene can inhibit the mass transport from the bulk solution to the electrode surface to benefit the CO_2 reduction instead of hydrogen evolution, thus greatly improving the selectivity of this catalyst.

Transition metal compound-based electrocatalysts can effectively reduce the overpotential and improve the energy efficiency of metal−CO_2 batteries.[106] Moreover, they can boost the electron transfer and tune the electronic structure of CO_2 to facilitate the conversion from CO_2 to selected value-added chemicals. Reducing the size of transition metal compound-based electrocatalysts becomes a feasible way to provide high numbers of active sites. For example, the nanostructure transition metal electrocatalysts show a strong ability to improve the electrochemical performance of both metal−CO_2 batteryies and CO_2 electrolysis. In addition, the design principles for transition metal compound-based electrocatalysts are based on morphological control and the selection of the supporting materials. Finally, the low price of transition metal compound catalysts increases the potential for large-scale applications compared with precious metal catalysts.[107]

https://doi.org/10.1021/acsenergylett.2c02445
ACS Energy Lett. 2023, 8, 1818−1838

SINGLE-ATOM ELECTROCATALYSTS

Single-atom electrocatalysts (SACs) with high metal utilization have attracted increasing attention and exhibit a wide range of applications, including material science, catalysis, and electrochemistry. Herein, M−N−C (M = Ni, Fe, Zn) is a typical model catalyst combining a single metal atom and N-doped carbon materials to explore an improved strategy for SACs. The local electronic densities of central metal atoms vary with coordination to the N atoms in SACs; thus, they can influence the adsorption of reaction intermediates and regulate the electrocatalytic activity. This can therefore boost the performance of both metal−CO_2 batteries and CO_2ER technologies. It was found that the electronic structure of the catalysts can be optimized by doping with nitrogen and/or adding non-noble metal species to carbon-based material. The adsorption capacity for specific reactants can then be enhanced. For instance, the metal atom will coordinate with the N atom to produce a stable M−N_x group. Its unique coordination structure and unsaturated coordination environment can improve the electrocatalytic performance. While Cu−N_x was found to have poor electrocatalytic performance, recent studies by Xu et al. constructed bimetallic active site systems by introducing a second atom (iron) to tailor the microstructure of electrocatalysts and change the chemical and electronic performance.[108] Figure 5a shows preparation procedures and microstructure for Fe−Cu−N−C. The new catalyst showed high surface adsorption state and promoted fission of the C=O bonds, owing to high densities of (bimetallic) active sites. The authors first introduced the Fe−Cu−N−C system to Na−CO_2 batteries and further investigated the mechanism of CO_2 activation. Their results show that a Na−CO_2 battery with this cathode catalyst has superior performance (voltage gap of 0.44 V and cyclability of 600 h), which is higher than those of other hybrid Na−CO_2PdNi batteries.

The synergistic effect between the isolated metal-N sites and graphitic N species can induce charge redistribution and enhance electron transport. The electrochemical performance of SACs has a strong connection to their local coordination environment. The electrocatalytic performance and selectivity of SACs highly relate to the electronic and geometric structure of their metal centers, which would be influenced by the coordination number. Therefore, it is important to regulate and control the coordination environment to improve electrocatalytic performance. Great progress has been made in constructing SACs; however, it is still challenging to precisely modulate coordination number while keeping the single-atom metal centers stable. Many methods have been proposed to solve the above issues. For example, Zheng et al. reported that one-step pyrolysis accompanied at high temperature can adjust the N coordination number.[109] The strategy of postsynthetic metal substitution is reported to demonstrate a controllable and convenient pathway for constructing single-atom Ni electrocatalysts. Meanwhile, it also can achieve the goal of synthesizing single Ni atoms with low coordination number on a N-doped carbon matrix, which is derived from a Zn-based MOF. Since the Zn−N bond is labile in acidic media, rich Zn−N_3 sites can form after the pyrolysis of the Zn-based MOF but will easily break down to leave Zn vacancies. Therefore, the authors succeeded in the fabrication for Ni−N_3−C catalyst. Then, Zn vacancies surrounded by 3 N atoms is refilled with a Ni atom to form Ni−N_3−C (Figure 5c). The theoretical calculation also shows that low-coordinated Ni atoms in Ni−N_3−C greatly benefit the formation of the *COOH intermediate, thus enhancing CO_2 reduction.

A series of Fe-based N-doped carbon samples act as good examples to demonstrate the optimization strategy while gaining a deeper understanding of the M−N−C structure. The advantage of Fe−N−C over other M−N−C catalysts is that it provides lower onset potential for CO_2 conversation. However, its electrocatalytic performance is not ideal because CO readily and strongly binds strongly to the Fe−N_x site, thus preventing its desorption and blocking the site. Different methods have been proposed to enhance the performance of CO_2 reduction, such as changing the morphology/structure of the loaded carbon matrix and adjusting the coordination structure/local environment around the iron atom. In addition, N doping points and intrinsic defects are also important. Defect-rich graphene with single-atom Fe−N_4 sites (DNG-SAFe) was developed. The associated studies demonstrated the specific role of defect-based carbon to ameliorate the Fe−N−C structure. This strategy combines the advantages of defect-rich carbon species and the atomic single Fe−N_4 site.[110] In this work, carbon-rich carbon nitride (C-*g*-C_3N_4) was used to provide carbon sources to fabricate intrinsic carbon defects with N dissipation. The electrochemical performance of DNG-SAFe is better than that of the electrocatalysts of DNG (only intrinsic defect sites) and NG-SAFe (only Fe−N_4 sites), indicating the advantages of combining intrinsic defect sites and Fe−N_4 sites.

Besides, the process of synthesizing isolated Fe active centers on N-doped carbon (Fe_1NC) reveals that the volcano relationship can guide the optimization of size for better electrochemical performance.[111] It shows the versatility of the gas diffusion process and paves the way for potential application of carbon-supported SACs through synthesizing a series of nanocarbon electrocatalysts (1D, 2D, and 3D). The presence of Fe−N_3 sites was predicted to reduce the energy barrier of *COOH formation as well as that associated with the following reaction. This was consistent with the high performance of the Zn−CO_2 battery; specifically, the power density and FE_{co} of the Zn−CO_2 battery assembled with cathode catalyst Fe_1NC can be beyond 500 mW/cm^2 and 95%, respectively. The Fe single atom surrounded with vacancy (FeN_3V) shows a modest energy barrier for all reaction states, starting from the formation of *COOH, to the conversion of *COOH to *CO, and the final desorption *CO to yield free, gas-phase CO. This indicates that introducing a vacancy for the Fe−N−C structure is highly beneficial.

Based on a similar idea, Fe−N_5 also shows the ability to improve FE_{co} as well compared to other catalysts. Li et al. constructed defective carbon nanofibers with a porous structure to support Fe−N_5 sites accompanied by N coordination (Fe−N_5/DPCF).[112] Figure 4c provides the synthetic process and the corresponding SEM images. The material is synthesized starting from zinc-based zeolitic imidazole frameworks (ZIF-8), in which the prepared precursor can be converted into Fe−N_x/PCF through an electrospinning method and thermal treatment. By integrating the advantages from dispersed Fe−N_5 sites and defective carbon, the catalyst Fe−N_5/DPCF can boost electronic localization to enhance the desorption of *CO and inhibit the hydrogen evolution reaction (HER). During pyrolysis, the Fe−N_5 active site is formed by axial coordination between Fe and the N atom of the adjacent nitrogen-doped carbon layer. In addition, selective removal of some unstable species, such as pyrrolic-N and pyridinic-N species, can promote the carbon support to produce more inherent defects.

https://doi.org/10.1021/acsenergylett.2c02445
ACS Energy Lett. 2023, 8, 1818−1838

The well-defined structure also exhibits advantages for improving the electrocatalytic performance of M−N−C. The novel Zn−N_4/C electrocatalyst with a twisted structure is obtained by a molten salt-assisted solid-phase method; the process is shown in Figure 4d.[113] The Zn−N_{3+1} active site is constructed by forming the coordination between a Zn^I atom and four N atoms, which shows an improved ability in comparison to other dispersed Zn−N−C electrocatalysts reported so far. The electrochemical results demonstrate the Zn−N_{3+1} active site supported by the carbon nanosheet can enhance dissociation of H_2O and facilitate protonation of *CO_2; this is reflected in a lower potential barrier for formation of the *COOH intermediate.

Because of the high density of exposed active sites, single-atom electrocatalysts (SACs) can be helpful for designing low-cost and high-performance cathodes. However, the harsh synthesis conditions and lengthy production process of previous SASCs increase the preparation cost of SASCs, presenting great obstacles for their industrial application. Therefore, simplifying the synthetic process while lowering the cost is urgently required. A single atom of Ru can be introduced onto the Co_3O_4 nanosheet array (Ru−Co_3O_4) by a cation exchange method. This method relies on mild conditions (350 °C and air atmosphere), which provides a facile way to obtain SACs (Figure 4b).[114] Ru−Co_3O_4 acts as dual-catalysts. The Co_3O_4 nanosheet array shows a greater ability to stabilize the mass transfer of CO_2/Li^+ and favors the formation of Li_2CO_3 compared to traditional carbon support. Ru atoms act as active sites for adjusting the nucleation behavior of the discharge products. It is worth mentioning that the inherent affinity of the electrocatalysts with $Li_2C_2O_4$ is improved by the use of Ru atoms. The change in morphology of the samples is also shown in Figure 4b, from smooth carbon fiber to Ru−Co_3O_4 with a slightly curled elliptical morphology.

SACs became promising materials to enhance the electrocatalytic performance; however, an important challenge still lies in their high onset potential. Inheriting the advantages of SACs, the diatomic site electrocatalysts (DASCs) can use two neighboring heterogeneous metal atoms for complementary functionalities and synergistic effects. Notably, electronic interaction between two neighboring atomic metals can control the binding energy with different intermediates. However, they still face the challenges of unclear working mechanisms and elaborate construction processes. To shed light on the synthesis process and electrocatalytic mechanism, high-density Ni and Fe atoms were anchored on N-doped graphene (NiFe-DASC); the resulting catalyst shows a stable and excellent electrochemical performance for CO_2-to-CO conversation (overpotential: 690 mV at 50.4 mA/cm^{-2}; FE: 94.5%).[115] The results are collected from the Zn−CO_2 battery loaded by a NiFe-DASC cathode. Furthermore, in-depth analysis of the electronic structure shows that the oxidation state of Fe, as the electrocatalytic center in the NiFe heteroatom pair, increases after coupling with the orbital of Ni, which reduces the binding strength to the intermediate. This study provides important guidance and insights for the rational design, working mechanism, and future applications of heterogeneous DASCs.

Regulating the binding energy of the intermediate can aid in achieving a high level of electrocatalytic activity and product selectivity simultaneously. The exciting result can be obtained by strain engineering.[119] Figure 5b offers a model for the aqueous rechargeable Zn−CO_2 battery with an s-PdNi/CNFs-1000 cathode. For the conversation from CO_2 to CO, strain engineering shows the powerful ability to adjust the binding energies of intermediate COOH* to regulate electrocatalytic properties, featuring high FE_{co} and selectivity. It is necessary to construct a well-understood and well-defined system to finely regulate lattice strain and to demonstrate the effect of strain for electrochemical CO_2 reduction. The strain PdNi NPs (s-PdNi) can be used as a model system to study the factors that determine strain effects. Characterization analysis of s-PdNi-800 shows a well-defined plane with an interatomic distance and even distribution of Pd and Ni (Figure 5b).

Selecting suitable SAC electrocatalysts for CO_2 electrocatalysis is still a hot topic.[120,121] The high efficiency and adjustable electrochemical environment/electronic structures offer an excellent platform for the CO_2 reduction reaction. Designing SAC electrocatalysts with low-cost, high-selectivity, and superior electrocatalytic activity plays an essential role in a large-scale application for CO_2 electrolysis. Zheng et al. reported a facile and scalable method to synthesize Ni SACs supported on carbon black with extraordinary performance.[122] One of the advantages of carbon black support is its onion-like structure and defective graphene layers that can effectively enhance CO_2 diffusion to increase the concentration of the reactants. In addition, carbon black can trap Ni atoms on the activated surface, which introduces electrocatalytic sites and coordination environment for CO_2 conversion. As a result, the individual Ni atom is well separated and has a strong anchor on the carbon black. This is consistent with the electrocatalytic performance. Single Ni atom electrocatalysts with carbon black achieve around 100% selectivity for CO production at a current density over 100 mA/cm^2.

The above-mentioned work shows the importance of supporting materials for SAC electrocatalysts. Cao's group designed varieties of carbon sphere supporting materials for Ni−N_4 electrocatalysts.[123] As a result, the Ni−N_4 supported by hollow mesoporous carbon spheres (Ni/HMCS-3-800) achieves a better electrocatalytic performance in which FE_{CO} is 95% (−0.7 to −1.1 V vs RHE) and turnover frequency value is 15608 h^{-1}. In addition, they extensively studied the influence of geometrical structures of the carbon supporting matrix. The electrochemical environment for SACs can be adjusted by the compactness as well as shell thickness of carbon spheres to activate CO_2. It shows enhanced CO_2 adsorption efficiency with the improved mesopore size. These works show a promising method for further exploration of the electrocatalytic performance of SACs electrocatalysts by designing optimized supporting materials.

A such, SACs, especially M−N−C-based SACs, have attracted a lot of researchers' attention due to their high activity and excellent selectivity.[124,125] The unique structure of the catalyst to expose as many atoms as possible results in the catalyst's high electrocatalytic activity. The unique properties of SACs can accelerate the degradation of the discharge products and accelerate the reaction kinetics of metal−CO_2 batteries, as well as promote the CO_2 electrolysis reaction. Meanwhile, the elaborate electronic structure and adjusted coordination environment of SACs also provide a viable way to further study the pathway of CO_2 reduction in the application of metal−CO_2 batteries and CO_2 electrolysis reaction.[126]

■ ORGANIC POLYMERS

Organic polymers, including phthalocyanine- and porphyrin-based polymers, MOFs, covalent organic frameworks (COFs), etc., are a novel class of heterogeneous catalysts.[127,128] The

https://doi.org/10.1021/acsenergylett.2c02445
ACS Energy Lett. 2023, 8, 1818−1838

porous structure of organic polymer electrocatalysts can increase the number of exposed active sites and facilitate mass transport, which improves both the cycle performance of metal−CO_2 batteries and the reaction kinetics of CO_2ER. In addition, high catalyst loading and excellent structural stability play vital roles in boosting the electrocatalytic performance for a longer time. All features are beneficial for organic polymer-based electrocatalysts to achieve a high level of CO_2 adsorption and conversion.[129] In the process of studying the electrocatalytic properties of organic polymers, how to precisely control the activity of the central metal atom has always been a research hotspot. For example, phthalocyanines are structurally related macrocyclic compounds with a highly conjugated π-electron system. Metal phthalocyanine (MPC) with transition metal center has the features of a well-defined coordination environment and tunable *d*-orbitals. Gong et al. modulated the electron-withdrawing effect of carbon defects and pyrrolic N to change the electronic structure of cobalt phthalocyanine (CoPc) supported by N-doped hollow carbon spheres (CoPc@NHCS).[130] Therefore, the authors were able to regulate the electronic structure of the metal to control the activity of heterogeneous macromolecule electrocatalysts. The results show that the Co electronic structure of CoPc is a key part of electrochemical CO_2ER, and the electron-withdrawing effect can boost the CO_2 activation and lower the barrier for *COOH formation on the Co^I metal sites.

Phthalocyanine is also designed and developed as the electrocatalyst for metal−CO_2 batteries. The conjugated cobalt polyphthalocyanine (CoPPc) featuring enhanced chemical and mechanical stability is synthesized by an easy microwave heating strategy to polymerize 1,2,4,5-etracyanobenzene and Co^{2+} (Figure 6c).[131] Compared with the CoPc monomer, the CoPPC shows a higher electrocatalytic activity for formation and decomposition of Li_2CO_3. According to the discharged and charged profile shown in Figure 6c (II and III), the Li−CO_2 battery can run for over 50 cycles at the current density 0.05 mA/cm^{-2} with a corresponding midcapacity voltage polarization (1.1 V) and energy efficiency (61%). The excellent chemical and physical stability as well as impressive electrocatalytic performance make the CoPPc polymer a promising catalyst for flexible Li−CO_2 batteries. In addition, this work demonstrates the potential for constructing flexible metal−CO_2 batteries by using an organometallic polymer catalyst.

Besides, MOFs/COFs with high-porosity materials, high thermal stability, versatility, and open channels provide the ability of powerful CO_2 capture and impressive electrocatalytic performance.[132] The unique structure can not only enhance the electrochemical kinetics but also provide an ideal example for studying ion and gas behavior during charge and discharge. Therefore, it is worth further exploring the application in the field of both metal−CO_2 batteries and electrochemical CO_2 reduction. It is found that different synthesis methods will affect the electrocatalytic performance of the polymer. Through fine-tuning of the internal strain on the Zn-porphyrin center, Zn MOF-based catalysts developed by a vapor-phase infiltration (VPI) method have improved intrinsic activity.[128] The VPI method can produce the Zn-porphyrin coordinated center on surface-bound MOFs, while internal stress is induced by excess ZnO growth inside MOFs. Compared with MOFs prepared by a transitional method, the strained MOFs can achieve almost 100% FE_{co} in CO_2 electrolysis. Ligand doping is also an effective strategy to improve the CO_2ER activity of MOFs; a ligand dopant featuring an electron-donating property can induce transfer of charge from the dopant molecule to the adjacent sp^2 C atom sites.[110] The formation of the *COOH intermediate benefits from this fast charge transfer from the active sites to the antibonding orbitals of CO_2, which promote activation.

Fortunately, increasing work shows that the classes of heterogeneous electrocatalysts that are suitable for metal−CO_2 batteries or CO_2 electrolysis could also provide feasible materials to advance the other application.

MOFs have been proven to be capable of CO_2 capture as well as gas separation. The ability to absorb CO_2 can be easily adjusted by tuning the pore size and functional groups of MOFs. In addition, benefiting from the well-aligned micropores provided by their ordered periodic structures, the growth of Li_2CO_3 forms a uniform nanostructure morphology, which can well avoids the agglomeration problem. The electrocatalytic metal center can be evenly dispersed in a highly porous skeleton, so the Li_2CO_3 can be efficiently decomposed. More importantly, the relation between structure and electrochemical performance can be precisely explained by systematically studying the behavior of metal centers and pore structures of MOFs (Figure 6a). Inspired by these ideas, Li et al. synthesized a series of porous MOFs.[133] Among these electrocatalysts, Mn-based MOFs show an impressive performance in Li−CO_2 batteries. The Mn_2(2,5-dioxido-1,4-benzenedicarboxylate), named Mn_2(dobdc), based cathode exhibits an excellent discharge capacity (18022 mAh/g at 50 mA/g). Low charging potential at about 4.0 V is achieved by $Mn(HCOO)_2$ after 50 cycles at a current density of 200 mA/g. The lower overpotential confirms the ability of the Mn(II) metal center to avoid high charging potential, indicating the importance of selecting suitable metal centers for MOF-based electrocatalysts. The high discharge capacity can be attributed to the increase of porosity and CO_2 adsorption of the MOF. Moreover, the energy loss of CO_2 evolution may be closely related to the effect of the isometric heat of CO_2 adsorbed by the MOF on charge polarization. The medium isosteric heat of CO_2 adsorption would be beneficial for obtaining lower charge polarization. These exciting results boost the development of MOF-based electrocatalyst to activate the metal−CO_2 electrochemistry, providing a clear guideline for designing highly efficient MOF-based electrocatalysts.

MOF electrocatalysts also provide the platform for CO_2 electrochemical reduction with an adjustable chemical environment. The Fe-porphyrin-based MOF with an electrostatic secondary-sphere exhibits an impressive electrocatalytic performance for CO_2 electrolysis.[135] *In situ* Raman spectra indicate that this Fe-porphyrin-based MOF with positively charged groups can stabilize the weakly bound CO intermediate. Therefore, the FE_{CO} can be improved effectively by steadily releasing the adsorbed CO. Meanwhile, the magnitude of the electrostatic field is adjustable by tuning the ionic strength of the electrolyte to achieve higher selectivity (about 100%).

COFs demonstrate excellent stability and strong competitiveness attributed to robust covalent linkage, especially when maintaining stability in other polymer materials is difficult. They can provide stable and atomically precise one-dimensional channels to enhance the transport of CO_2/Li^+ diffusion and improve the electrochemical reactions kinetics. As shown in

https://doi.org/10.1021/acsenergylett.2c02445
ACS Energy Lett. 2023, 8, 1818−1838

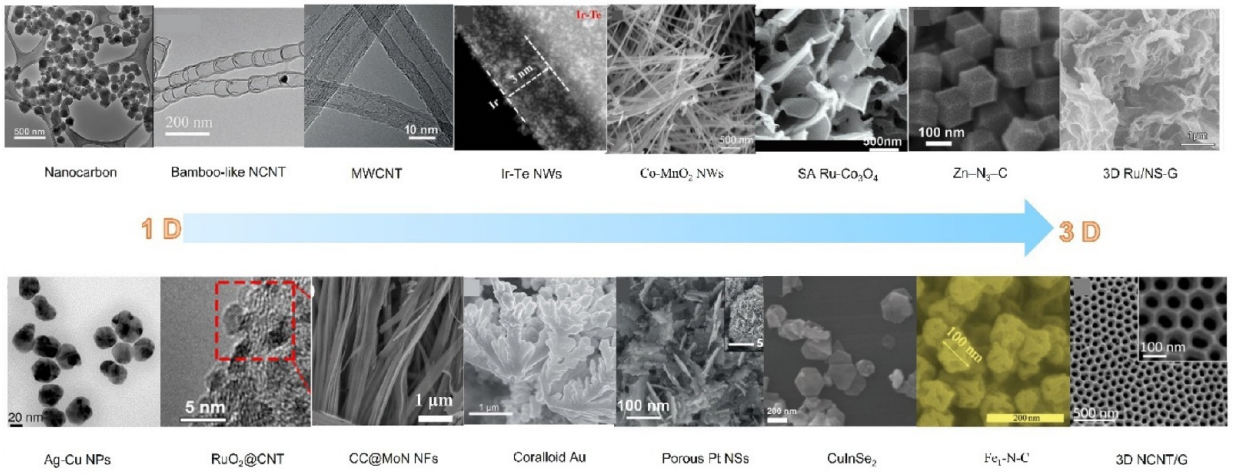

Figure 7. Variety of morphologies of electrocatalysts for metal−CO_2 batteries and CO_2 electrolysis. The inserted graphics are adapted with permission from ref 28, Wiley 2018; ref 68, American Chemical Society 2020; ref 71, Wiley 2019; ref 73, Elsevier 2020; ref 74, Wiley 2016; ref 75, American Chemical Society 2020; ref 84, American Chemical Society 2019; ref 85, Elsevier 2021; ref 89, American Chemical Society 2019; ref 103, Wiley 2019; ref 114, Wiley 2021; ref 117, Wiley 2022; ref 118, The Royal Society of Chemistry 2021.

Figure 6b, COFs and the traditional Ru@CNT can act as CO_2 absorbers and diffusion layer for ion and gas, which ensure that the Li−CO_2 battery has high energy capacity (27 348 mAh g^{-1} at 200 mA g^{-1}).[134] The COF-based electrocatalysts with excellent properties of ion/gas transport offer a platform for understanding and exploring the full potential of metal−CO_2 batteries.

In addition, Guo et al. reported cooperative cobalt-protoporphyrin (CoPP) on the metal−organic layers (MOLs) for CO_2 electrolysis.[136] The ultrathin MOLs are regarded as a novel type of functional molecular materials due to high conductivity. It also provides a shorter path for electron migration and movement. In particular, the microenvironment of electrocatalytic centers can be controlled by modifying the surface of the MOLs. In this case, the 2D MOLs act as a substrate that can precisely adjust the microenvironment of the electrocatalyst CoPP to further improve the electrochemical performance of CO_2 conversion. In addition, the CoPP sites and pyridinium moiety on MOLs can both activate CO_2 with the formation of [pyH^+_-O_2C-CoPP], thus improving the CO_{FE} and inhibiting hydrogen evolution. Therefore, this work provides an adjustable platform of MOLs to optimize product selectivity and understand the electrocatalytic processes of CO_2 conversion.

In conclusion, organic polymer electrocatalysts became one of the burgeoning electrocatalysts for metal−CO_2 batteries and CO_2 electrolysis due to the unique tunable structure and excellent electrocatalytic performance.[137,138] In metal−CO_2 batteries, the (metallo)organic polymer electrocatalysts can boost the reaction kinetic and increase energy efficiency through facilitating the gas/ion transfer. In addition, the high surface area, controlled functionality, and exciting stability play important roles in enhancing the CO_2 adsorption and electron movement.

OUTLOOK

Metal−CO_2 batteries and CO_2 electrolysis both rely on efficient CO_2ER and have similar reaction mechanisms. However, the reaction conditions, reaction products, and main challenges are different for these two applications. Fortunately, increasing work shows that the classes of heterogeneous electrocatalysts that are suitable for one application could also provide feasible materials to advance the other application.[139−142] Notably, using advanced technology, we can further explore the performance of heterogeneous electrocatalysts. For example, machine learning and artificial intelligence can help select and optimize the electrocatalytic performance of heterogeneous electrocatalysts.[143,144] In addition, advanced characterization methods act as useful tools to study the mechanism of CO_2ER.[145] However, the development of the heterogeneous electrocatalysts still has some limitations; therefore, we can summarize the challenges faced as well as the corresponding strategies as follows:

(1) The low surface area of many electrocatalysts hinders large-scale application. This not only reduces the ability of the catalyst to improve the cycling performance of metal−CO_2 batteries but also limits the efficiency of electron transfer during the process of CO_2 electrolysis. Designing nanostructured electrocatalysts to increase the surface area, thus providing more active sites, has become an effective method to tackle this problem (Figure 7). For example, rechargeable Na−CO_2 batteries assembled with a $ZnCo_2O_4$ nanorod cathode exhibit higher cycle number (150 cycles at 100 mA g^{-1}) and lower charge overpotential (3.8 V). This result can be attributed to the highly efficient decomposition of the discharge product and fast electron transfer.[146]

(2) Finding feasible and low-cost methods to synthesize the desired electrocatalysts always catches the attention of researchers. For example, MOFs owning tailorable composition and structure provide a promising way to control the coordination microenvironment of SACs. However, different doping metals will have different effects on the formation of the MOF and its properties. Judicious selection of MOF precursors is needed to design different metal-based systems. Therefore, this strategy might be difficult to apply for large-scale application. Some additional drawbacks render this method not ideal. One issue is that the carbonization of the MOF and the formation and aggregation of single atoms may occur simultaneously. Therefore, some complex synthesis parameters, such as pyrolysis temperature and metal loading, can interact with each other in the one-step pyrolysis process, resulting in a lack of understanding of the specific roles of each factor. Zhang et al. reported that accurate control of the coordination

https://doi.org/10.1021/acsenergylett.2c02445
ACS Energy Lett. 2023, 8, 1818−1838

surroundings followed by a postsynthetic metal substitution method can yield desired products easily, which provides a promising way to deal with this problem.[147]

(3) Understanding the electrocatalytic mechanism of CO_2ER is pivotal for the development of the next generation of heterogeneous electrocatalysts. Taking SACs as an example, elaborately adjusting the behavior of metal atoms and the electronic structure is regard as an important way to achieve high electrocatalytic performance. Therefore, Ru atom/Ru−N_4 sites supported by a carbon nanobox substrate elucidate the relationship between electronic structure and properties of the electrocatalysts. The neighboring Ru_{AC} species show a strong ability to adjust active site Ru−N_4 to increase the binding energy between active sites and reaction intermediates, which can effectively lower the energy barrier of the rate-determining step of CO_2 conversion.[125] In addition, the accelerated process of carbon desorption is also good enough to avoid poisoning problems, allowing a steady uptake of CO_2 over time.

(4) Designing suitable heterogeneous electrocatalysts for conversion of CO_2 to higher-order carbon products (C_{2+}) can promote the production of value-added chemicals. However, the possible reaction pathways toward C_{2+} products need to be further explored. Besides, typical electrocatalysts need high overpotential to achieve excellent reaction rates, and the competition of the hydrogen evolution reaction must be considered. Fortunately, copper-based heterogeneous electrocatalysts can provide a great platform to study the factors affecting the reaction.[148] For example, the experimental results show that CO* dimerization to OCCO* on Cu(100) is the key step for producing C_{2+} products.[149] Therefore, it is worth exploring excellent heterogeneous electrocatalysts to achieve high-efficiency CO_2-to-C_{2+} products based on Cu-based electrocatalysts.

(5) Compared with heterogeneous electrocatalysts, homogeneous electrocatalysts have higher selectivity, but their activity and stability make it difficult to meet industrial requirements. The recovery process of homogeneous electrocatalysts is very complex, which is also one of the obstacles for large-scale applications.[150] Therefore, designing hybrid homogeneous−heterogeneous electrocatalysts might be a promising way to combine the advantages of both heterogeneous and homogeneous electrocatalysts.

Overall, heterogeneous electrocatalysts (carbon-based, noble metal-based, transition metal compounds, single-atom, and organic polymer electrocatalysts) are promising ways to further the development of both metal−CO_2 batteries and CO_2 electrolysis based on electrochemical methods. We hope that this Focus Review can provide a new understanding of the connection of heterogeneous electrocatalysts in both applications. We hope to inspire researchers to design and develop electrocatalysts with higher surface area, better electrocatalytic activity, and superior stability. Next-generation heterogeneous electrocatalysts can help realize metal−CO_2 batteries and CO_2 electrolysis applications that could become crucial for overcoming carbon emissions.

AUTHOR INFORMATION

Corresponding Authors

Xiao-Dong Zhou − *Department of Chemical Engineering, Institute for Materials Research and Innovations, University of Louisiana at Lafayette, Louisiana 70504, United States;* orcid.org/0000-0001-9934-9429; Email: xiao-dong.zhou@louisiana.edu

Shuya Wei − *Department of Chemical and Biological Engineering, University of New Mexico, Albuquerque, New Mexico 87131, United States;* orcid.org/0000-0001-9269-1950; Email: swei@unm.edu

Authors

Jianda Wang − *Department of Chemical and Biological Engineering, University of New Mexico, Albuquerque, New Mexico 87131, United States*

Barbara Marchetti − *Department of Chemical Engineering, Institute for Materials Research and Innovations, University of Louisiana at Lafayette, Louisiana 70504, United States;* orcid.org/0000-0002-0661-9029

Complete contact information is available at: https://pubs.acs.org/10.1021/acsenergylett.2c02445

Notes

The authors declare no competing financial interest.

Biographies

Jianda Wang received his B.S. degree from Yangzhou university in 2020. He is currently a graduate student in Dr. Shuya Wei's group at the University of New Mexico. His research interests include developing advanced cathode materials for Li−CO_2 and Na−CO_2 batteries.

Dr. Barbara Marchetti received her Ph.D. from University of Bristol. She is now an instructor of chemistry at University of Louisiana at Lafayette. Her research focuses on experimental studies of the spectroscopy and photochemistry of (bio)molecules in bulk complex environments.

Professor Xiao-Dong Zhou is the Stuller Endowed Chair in the Chemical Engineering Department and the Director of the Institute for Materials Research and Innovations at the University of Louisiana at Lafayette. His research focuses on materials and interfaces for energy systems, including batteries, fuel cells, and electrolyzers. Website: https://www.zhoulab.com

Dr. Shuya Wei is an assistant professor in the Department of Chemical & Biological Engineering at UNM. She received her Ph.D. in Chemical Engineering from Cornell University, and she was a postdoctoral fellow at Massachusetts Institute of Technology. Her research interests include energy storage and carbon capture. Website: https://www.sweigroup.com

ACKNOWLEDGMENTS

This work was supported by the National Science Foundation Award Number 2119688. S.W. acknowledges financial support from the University of New Mexico startup fund.

REFERENCES

(1) Zhu, S.; Delmo, E. P.; Li, T.; Qin, X.; Tian, J.; Zhang, L.; Shao, M. Recent Advances in Catalyst Structure and Composition Engineering Strategies for Regulating CO_2 Electrochemical Reduction. *Adv. Mater.* **2021**, *33* (50), 2005484.

(2) Liang, S.; Huang, L.; Gao, Y.; Wang, Q.; Liu, B. Electrochemical Reduction of CO_2 to CO over Transition Metal/N-Doped Carbon Catalysts: The Active Sites and Reaction Mechanism. *Adv. Sci.* **2021**, *8* (24), 2102886.

(3) Li, S.; Nagarajan, A. V.; Alfonso, D. R.; Sun, M.; Kauffman, D. R.; Mpourmpakis, G.; Jin, R. Boosting CO_2 Electrochemical Reduction with Atomically Precise Surface Modification on Gold Nanoclusters. *Angew. Chemie - Int. Ed.* **2021**, *60* (12), 6351−6356.

(4) Lyu, Z.; Zhu, S.; Xie, M.; Zhang, Y.; Chen, Z.; Chen, R.; Tian, M.; Chi, M.; Shao, M.; Xia, Y. Controlling the Surface Oxidation of Cu Nanowires Improves Their Catalytic Selectivity and Stability toward

C2+ Products in CO_2 Reduction. *Angew. Chemie - Int. Ed.* **2021**, *60* (4), 1909−1915.
(5) Scholten, F.; Nguyen, K. L. C.; Bruce, J. P.; Heyde, M.; Roldan Cuenya, B. Identifying Structure-Selectivity Correlations in the Electrochemical Reduction of CO_2: A Comparison of Well-Ordered Atomically Clean and Chemically Etched Copper Single-Crystal Surfaces. *Angew. Chemie - Int. Ed.* **2021**, *60* (35), 19169−19175.
(6) Liu, Y.; Zhao, S.; Wang, D.; Chen, B.; Zhang, Z.; Sheng, J.; Zhong, X.; Zou, X.; Jiang, S. P.; Zhou, G.; Cheng, H. M. Toward an Understanding of the Reversible Li-CO_2 Batteries over Metal-N4-Functionalized Graphene Electrocatalysts. *ACS Nano* **2022**, *16* (1), 1523−1532.
(7) Guan, D. H.; Wang, X. X.; Li, F.; Zheng, L. J.; Li, M. L.; Wang, H. F.; Xu, J. J. All-Solid-State Photo-Assisted Li-CO_2 Battery Working at an Ultra-Wide Operation Temperature. *ACS Nano* **2022**, *16* (8), 12364−12376.
(8) Li, Y.; Zhou, J.; Zhang, T.; Wang, T.; Li, X.; Jia, Y.; Cheng, J.; Guan, Q.; Liu, E.; Peng, H.; Wang, B. Highly Surface-Wrinkled and N-Doped CNTs Anchored on Metal Wire: A Novel Fiber-Shaped Cathode toward High-Performance Flexible Li-CO_2 Batteries. *Adv. Funct. Mater.* **2019**, *29* (12), 1808117.
(9) Zhang, B.; Jiao, Y.; Chao, D.; Ye, C.; Wang, Y.; Davey, K.; Liu, H.; Dou, S.; Qiao, S. Targeted Synergy between Adjacent Co Atoms on Graphene Oxide as an Efficient New Electrocatalyst for Li-CO_2 Batteries. *Adv. Funct. Mater.* **2019**, *29* (49), 1904206.
(10) Frank, S.; Svensson Grape, E.; Bøjesen, E. D.; Larsen, R.; Lamagni, P.; Catalano, J.; Inge, A. K.; Lock, N. Exploring the Influence of Atomic Level Structure, Porosity, and Stability of Bismuth(Iii) Coordination Polymers on Electrocatalytic CO_2 reduction. *J. Mater. Chem. A* **2021**, *9* (46), 26298−26310.
(11) Corbin, N.; Zeng, J.; Williams, K.; Manthiram, K. Heterogeneous Molecular Catalysts for Electrocatalytic CO_2 Reduction. *Nano Res.* **2019**, *12* (9), 2093−2125.
(12) Ding, T.; Liu, X.; Tao, Z.; Liu, T.; Chen, T.; Zhang, W.; Shen, X.; Liu, D.; Wang, S.; Pang, B.; Wu, D.; Cao, L.; Wang, L.; Liu, T.; Li, Y.; Sheng, H.; Zhu, M.; Yao, T. Atomically Precise Dinuclear Site Active toward Electrocatalytic CO_2 Reduction. *J. Am. Chem. Soc.* **2021**, *143* (30), 11317−11324.
(13) Koenig, J. D. B.; Dubrawski, Z. S.; Rao, K. R.; Willkomm, J.; Gelfand, B. S.; Risko, C.; Piers, W. E.; Welch, G. C. Lowering Electrocatalytic CO_2 Reduction Overpotential Using N-Annulated Perylene Diimide Rhenium Bipyridine Dyads with Variable Tether Length. *J. Am. Chem. Soc.* **2021**, *143* (40), 16849−16864.
(14) Yu, S.; Kim, D.; Qi, Z.; Louisia, S.; Li, Y.; Somorjai, G. A.; Yang, P. Nanoparticle Assembly Induced Ligand Interactions for Enhanced Electrocatalytic CO_2 Conversion. *J. Am. Chem. Soc.* **2021**, *143* (47), 19919−19927.
(15) Sun, X.; Tuo, Y.; Ye, C.; Chen, C.; Lu, Q.; Li, G.; Jiang, P.; Chen, S.; Zhu, P.; Ma, M.; Zhang, J.; Bitter, J. H.; Wang, D.; Li, Y. Phosphorus Induced Electron Localization of Single Iron Sites for Boosted CO_2 Electroreduction Reaction. *Angew. Chemie - Int. Ed.* **2021**, *60* (44), 23614−23618.
(16) Zulfiqar, S.; Mantione, D.; El Tall, O.; Ruipérez, F.; Sarwar, M. I.; Rothenberger, A.; Mecerreyes, D. Pyridinium Containing Amide Based Polymeric Ionic Liquids for CO_2 /CH 4 Separation. *ACS Sustain. Chem. Eng.* **2019**, *7* (12), 10241−10247.
(17) Zhang, J.; Wang, F.; Qi, G.; Cheng, J.; Chen, L.; Liu, H.; Wang, B. Rechargeable Li−CO_2 Batteries with Graphdiyne as Efficient Metal-Free Cathode Catalysts. *Adv. Funct. Mater.* **2021**, *31* (26), 2101423.
(18) Wang, Y.; Zhou, J.; Lin, C.; Chen, B.; Guan, Z.; Ebrahim, A. M.; Qian, G.; Ye, C.; Chen, L.; Ge, Y.; Yun, Q.; Wang, X.; Zhou, X.; Wang, G.; Li, K.; Lu, P.; Ma, Y.; Xiong, Y.; Wang, T.; Zheng, L.; Chu, S.; Chen, Y.; Wang, B.; Lee, C.; Liu, Y.; Zhang, Q.; Fan, Z. Decreasing the Overpotential of Aprotic Li-CO_2 Batteries with the In-Plane Alloy Structure in Ultrathin 2D Ru-Based Nanosheets. *Adv. Funct. Mater.* **2022**, *32* (30), 2202737.
(19) Wang, F.; Li, Y.; Xia, X.; Cai, W.; Chen, Q.; Chen, M. Metal-CO_2 Electrochemistry: From CO_2 Recycling to Energy Storage. *Adv. Energy Mater.* **2021**, *11* (25), 2100667.
(20) Liu, L.; Qin, Y.; Wang, K.; Mao, H.; Wu, H.; Yu, W.; Zhang, D.; Zhao, H.; Wang, H.; Wang, J.; Xiao, C.; Su, Y.; Ding, S. Rational Design of Nanostructured Metal/C Interface in 3D Self-Supporting Cellulose Carbon Aerogel Facilitating High-Performance Li-CO_2 Batteries. *Adv. Energy Mater.* **2022**, *12* (20), 2103681.
(21) Mu, X.; Pan, H.; He, P.; Zhou, H. Li-CO_2 and Na-CO_2 Batteries: Toward Greener and Sustainable Electrical Energy Storage. *Adv. Mater.* **2019**, *32* (27), 1903790.
(22) Tao, Z.; Rooney, C. L.; Liang, Y.; Wang, H. Accessing Organonitrogen Compounds via C-N Coupling in Electrocatalytic CO_2 Reduction. *J. Am. Chem. Soc.* **2021**, *143* (47), 19630−19642.
(23) Wang, J.; Xiao, X.; Liu, Y.; Pan, K.; Pang, H.; Wei, S. The Application of CeO_2 -Based Materials in Electrocatalysis. *J. Mater. Chem. A* **2019**, *7* (30), 17675−17702.
(24) Kim, J.-Y.; Hong, D.; Lee, J.-C.; Kim, H. G.; Lee, S.; Shin, S.; Kim, B.; Lee, H.; Kim, M.; Oh, J.; Lee, G.-D.; Nam, D.-H.; Joo, Y.-C. Quasi-Graphitic Carbon Shell-Induced Cu Confinement Promotes Electrocatalytic CO_2 Reduction toward C2+ Products. *Nat. Commun.* **2021**, *12* (1), 3765.
(25) Yao, D.; Tang, C.; Vasileff, A.; Zhi, X.; Jiao, Y.; Qiao, S. Z. The Controllable Reconstruction of Bi-MOFs for Electrochemical CO_2 Reduction through Electrolyte and Potential Mediation. *Angew. Chemie - Int. Ed.* **2021**, *60* (33), 18178−18184.
(26) Fan, L.; Shen, H.; Ji, D.; Xing, Y.; Tao, L.; Sun, Q.; Guo, S. Biaxially Compressive Strain in Ni/Ru Core/Shell Nanoplates Boosts Li-CO_2 Batteries. *Adv. Mater.* **2022**, *34* (30), 2204134.
(27) Zhang, Z.; Zheng, Y.; Qian, L.; Luo, D.; Dou, H.; Wen, G.; Yu, A.; Chen, Z. Emerging Trends in Sustainable CO_2 -Management Materials. *Adv. Mater.* **2022**, *34* (29), 2201547.
(28) Xie, J.; Wang, X.; Lv, J.; Huang, Y.; Wu, M.; Wang, Y.; Yao, J. Reversible Aqueous Zinc-CO_2 Batteries Based on CO_2-HCOOH Interconversion. *Angew. Chemie - Int. Ed.* **2018**, *57* (52), 16996−17001.
(29) Wang, J.; Cheng, T.; Fenwick, A. Q.; Baroud, T. N.; Rosas-Hernández, A.; Ko, J. H.; Gan, Q.; Goddard, W. A.; Grubbs, R. H. Selective CO_2 Electrochemical Reduction Enabled by a Tricomponent Copolymer Modifier on a Copper Surface. *J. Am. Chem. Soc.* **2021**, *143* (7), 2857−2865.
(30) Xie, J.; Zhou, Z.; Wang, Y. Metal-CO_2 Batteries at the Crossroad to Practical Energy Storage and CO_2 Recycle. *Adv. Funct. Mater.* **2020**, *30* (9), 1908285.
(31) He, Y.; Ma, D.; Zhou, S.; Zhang, M.; Tian, J.; Zhu, Q. Integrated 3D Open Network of Interconnected Bismuthene Arrays for Energy-Efficient and Electrosynthesis-Assisted Electrocatalytic CO_2 Reduction. *Small* **2022**, *18* (1), 2105246.
(32) Li, M.; Yan, C.; Ramachandran, R.; Lan, Y.; Dai, H.; Shan, H.; Meng, X.; Cui, D.; Wang, F.; Xu, Z. X. Non-Peripheral Octamethyl-Substituted Cobalt Phthalocyanine Nanorods Supported on N-Doped Reduced Graphene Oxide Achieve Efficient Electrocatalytic CO_2 Reduction to CO. *Chem. Eng. J.* **2022**, *430* (P3), 133050.
(33) Gong, S.; Wang, W.; Xiao, X.; Liu, J.; Wu, C.; Lv, X. Elucidating Influence of the Existence Formation of Anchored Cobalt Phthalocyanine on Electrocatalytic CO_2 -to-CO Conversion. *Nano Energy* **2021**, *84*, 105904.
(34) Wu, Z. Z.; Gao, F. Y.; Gao, M. R. Regulating the Oxidation State of Nanomaterials for Electrocatalytic CO_2 reduction. *Energy Environ. Sci.* **2021**, *14* (3), 1121−1139.
(35) Jin, S.; Hao, Z.; Zhang, K.; Yan, Z.; Chen, J. Advances and Challenges for the Electrochemical Reduction of CO_2 to CO: From Fundamentals to Industrialization. *Angew. Chem.* **2021**, *133* (38), 20795−20816.
(36) Wu, Y.; Liang, Y.; Wang, H. Heterogeneous Molecular Catalysts of Metal Phthalocyanines for Electrochemical CO_2 Reduction Reactions. *Acc. Chem. Res.* **2021**, *54* (16), 3149−3159.
(37) Zhang, W.; Yang, S.; Jiang, M.; Hu, Y.; Hu, C.; Zhang, X.; Jin, Z. Nanocapillarity and Nanoconfinement Effects of Pipet-like Bismuth@Carbon Nanotubes for Highly Efficient Electrocatalytic CO_2 Reduction. *Nano Lett.* **2021**, *21* (6), 2650−2657.
(38) Devi, N.; Williams, C. K.; Chaturvedi, A.; Jiang, J. Homogeneous Electrocatalytic CO_2 Reduction Using a Porphyrin Complex with

https://doi.org/10.1021/acsenergylett.2c02445
ACS Energy Lett. 2023, 8, 1818−1838

Flexible Triazole Units in the Second Coordination Sphere. *ACS Appl. Energy Mater.* **2021**, *4* (4), 3604−3611.
(39) Wan, X.; Wang, J.; Wang, Q. Ligand-Protected Au 55 with a Novel Structure and Remarkable CO_2 Electroreduction Performance. *Angew. Chem.* **2021**, *133* (38), 20916−20921.
(40) Mu, X.; Pan, H.; He, P.; Zhou, H. Li-CO_2 and Na-CO_2 Batteries: Toward Greener and Sustainable Electrical Energy Storage. *Adv. Mater.* **2019**, *32* (27), 1903790.
(41) Liu, H.; Shi, S.; Wang, Z.; Han, Y.; Huang, W. Recent Advances in Metal-Gas Batteries with Carbon-Based Nonprecious Metal Catalysts. *Small* **2022**, *18* (10), 2103747.
(42) Jin, Y.; Liu, Y.; Song, L.; Yu, J.; Li, K.; Zhang, M.; Wang, J. Interfacial Engineering in Hollow NiS2/FeS2-NSGA Heterostructures with Efficient Catalytic Activity for Advanced Li-CO_2 Battery. *Chem. Eng. J.* **2022**, *430* (P3), 133029.
(43) Zhang, P. F.; Sheng, T.; Zhou, Y.; Wu, Y. J.; Xiang, C. C.; Lin, J. X.; Li, Y. Y.; Li, J. T.; Huang, L.; Sun, S. G. Li-CO_2/O_2 Battery Operating at Ultra-Low Overpotential and Low O_2 Content on Pt/CNT Catalyst. *Chem. Eng. J.* **2022**, *448* (June), 137541.
(44) Ezeigwe, E. R.; Dong, L.; Manjunatha, R.; Zuo, Y.; Deng, S. Q.; Tan, M.; Yan, W.; Zhang, J.; Wilkinson, D. P. A Review of Lithium-O_2/CO_2 and Lithium-CO_2 Batteries: Advanced Electrodes/Materials/Electrolytes and Functional Mechanisms. *Nano Energy* **2022**, *95*, 106964.
(45) Guo, X.; Xu, S. M.; Zhou, H.; Ren, Y.; Ge, R.; Xu, M.; Zheng, L.; Kong, X.; Shao, M.; Li, Z.; Duan, H. Engineering Hydrogen Generation Sites to Promote Electrocatalytic CO_2 Reduction to Formate. *ACS Catal.* **2022**, *12* (17), 10551−10559.
(46) Zhang, P. F.; Zhang, J. Y.; Sheng, T.; Lu, Y. Q.; Yin, Z. W.; Li, Y. Y.; Peng, X. X.; Zhou, Y.; Li, J. T.; Wu, Y. J.; Lin, J. X.; Xu, B.-B.; Qu, X. M.; Huang, L.; Sun, S. G. Synergetic Effect of Ru and NiO in the Electrocatalytic Decomposition of Li2CO3 to Enhance the Performance of a Li-CO_2/O_2 Battery. *ACS Catal.* **2020**, *10* (2), 1640−1651.
(47) Pham, T. H. M.; Zhang, J.; Li, M.; Shen, T.; Ko, Y.; Tileli, V.; Luo, W.; Züttel, A. Enhanced Electrocatalytic CO_2 Reduction to C 2+ Products by Adjusting the Local Reaction Environment with Polymer Binders. *Adv. Energy Mater.* **2022**, *12* (9), 2103663.
(48) Xi, D.; Li, J.; Low, J.; Mao, K.; Long, R.; Li, J.; Dai, Z.; Shao, T.; Zhong, Y.; Li, Y.; Li, Z.; Loh, X. J.; Song, L.; Ye, E.; Xiong, Y. Limiting the Uncoordinated N Species in M-N x Single-Atom Catalysts toward Electrocatalytic CO_2 Reduction in Broad Voltage Range. *Adv. Mater.* **2022**, *34* (25), 2104090.
(49) Yuan, J.; Chen, S.; Zhang, Y.; Li, R.; Zhang, J.; Peng, T. Structural Regulation of Coupled Phthalocyanine-Porphyrin Covalent Organic Frameworks to Highly Active and Selective Electrocatalytic CO_2 Reduction. *Adv. Mater.* **2022**, *34* (30), 2203139.
(50) Wang, Y.; Li, Y.; Liu, J.; Dong, C.; Xiao, C.; Cheng, L.; Jiang, H.; Jiang, H.; Li, C. BiPO 4 -Derived 2D Nanosheets for Efficient Electrocatalytic Reduction of CO_2 to Liquid Fuel. *Angew. Chem.* **2021**, *133* (14), 7759−7763.
(51) Xu, S. M.; Ren, Z. C.; Liu, X.; Liang, X.; Wang, K. X.; Chen, J. S. Carbonate Decomposition: Low-Overpotential Li-CO_2 Battery Based on Interlayer-Confined Monodisperse Catalyst. *Energy Storage Mater.* **2018**, *15*, 291−298.
(52) Pipes, R.; He, J.; Bhargav, A.; Manthiram, A. Efficient Li-CO_2 Batteries with Molybdenum Disulfide Nanosheets on Carbon Nanotubes as a Catalyst. *ACS Appl. Energy Mater.* **2019**, *2* (12), 8685−8694.
(53) Wu, M.; Kim, J. Y.; Park, H.; Kim, D. Y.; Cho, K. M.; Lim, E.; Chae, O. B.; Choi, S.; Kang, Y.; Kim, J.; Jung, H. T. Understanding Reaction Pathways in High Dielectric Electrolytes Using β-Mo_2C as a Catalyst for Li-CO_2 Batteries. *ACS Appl. Mater. Interfaces* **2020**, *12* (29), 32633−32641.
(54) Liu, L.; Zhang, L.; Wang, K.; Wu, H.; Mao, H.; Li, L.; Sun, Z.; Lu, S.; Zhang, D.; Yu, W.; Ding, S. Understanding the Dual-Phase Synergy Mechanism in Mn2O3-Mn3O4Catalyst for Efficient Li-CO_2 Batteries. *ACS Appl. Mater. Interfaces* **2020**, *12* (30), 33846−33854.
(55) Zhang, H.; Cheng, W.; Luan, D.; Lou, X. W. Atomically Dispersed Reactive Centers for Electrocatalytic CO_2 Reduction and Water Splitting. *Angew. Chemie - Int. Ed.* **2021**, *60* (24), 13177−13196.
(56) Liu, J.; Yang, D.; Zhou, Y.; Zhang, G.; Xing, G.; Liu, Y.; Ma, Y.; Terasaki, O.; Yang, S.; Chen, L. Tricycloquinazoline-Based 2D Conductive Metal-Organic Frameworks as Promising Electrocatalysts for CO_2 Reduction. *Angew. Chemie - Int. Ed.* **2021**, *60* (26), 14473−14479.
(57) Xie, W.; Li, H.; Cui, G.; Li, J.; Song, Y.; Li, S.; Zhang, X.; Lee, J. Y.; Shao, M.; Wei, M. NiSn Atomic Pair on an Integrated Electrode for Synergistic Electrocatalytic CO_2 Reduction. *Angew. Chem.* **2021**, *133* (13), 7458−7464.
(58) Jia, L.; Sun, M.; Xu, J.; Zhao, X.; Zhou, R.; Pan, B.; Wang, L.; Han, N.; Huang, B.; Li, Y. Phase-Dependent Electrocatalytic CO_2 Reduction on Pd 3 Bi Nanocrystals. *Angew. Chem.* **2021**, *133* (40), 21909−21913.
(59) Thoka, S.; Tsai, C. M.; Tong, Z.; Jena, A.; Wang, F. M.; Hsu, C. C.; Chang, H.; Hu, S. F.; Liu, R. S. Comparative Study of Li-CO_2 and Na-CO_2 Batteries with Ru@CNT as a Cathode Catalyst. *ACS Appl. Mater. Interfaces* **2021**, *13* (1), 480−490.
(60) Chen, C. J.; Huang, C. S.; Huang, Y. C.; Wang, F. M.; Wang, X. C.; Wu, C. C.; Chang, W. S.; Dong, C. L.; Yin, L. C.; Liu, R. S. Catalytically Active Site Identification of Molybdenum Disulfide as Gas Cathode in a Nonaqueous Li-CO_2 Battery. *ACS Appl. Mater. Interfaces* **2021**, *13* (5), 6156−6167.
(61) Liu, Q.; Hu, Z.; Li, L.; Li, W.; Zou, C.; Jin, H.; Wang, S.; Chou, S. L. Facile Synthesis of Birnessite δ-MnO_2 and Carbon Nanotube Composites as Effective Catalysts for Li-CO_2 Batteries. *ACS Appl. Mater. Interfaces* **2021**, *13* (14), 16585−16593.
(62) Zhu, Q. C.; He, Z. R.; Mao, D. Y.; Lu, W. N.; Yi, S. L.; Wang, K. X. Nanofibrous Cathode Catalysts with MoC Nanoparticles Embedded in N-Rich Carbon Shells for Low-Overpotential Li-CO_2 Batteries. *ACS Appl. Mater. Interfaces* **2022**, *14* (33), 38090−38097.
(63) Zhao, K.; Quan, X. Carbon-Based Materials for Electrochemical Reduction of CO_2 to C2+oxygenates: Recent Progress and Remaining Challenges. *ACS Catal.* **2021**, *11* (4), 2076−2097.
(64) Wang, J.; Tan, H.; Zhu, Y.; Chu, H.; Chen, H. M. Linking the Dynamic Chemical State of Catalysts with the Product Profile of Electrocatalytic CO_2 Reduction. *Angew. Chem.* **2021**, *133* (32), 17394−17407.
(65) Pan, Y.; Lin, R.; Chen, Y.; Liu, S.; Zhu, W.; Cao, X.; Chen, W.; Wu, K.; Cheong, W.-C.; Wang, Y.; Zheng, L.; Luo, J.; Lin, Y.; Liu, Y.; Liu, C.; Li, J.; Lu, Q.; Chen, X.; Wang, D.; Peng, Q.; Chen, C.; Li, Y. Design of Single-Atom Co-N 5 Catalytic Site: A Robust Electrocatalyst for CO_2 Reduction with Nearly 100% CO Selectivity and Remarkable Stability. *J. Am. Chem. Soc.* **2018**, *140* (12), 4218−4221.
(66) Wu, Z.; Wu, H.; Cai, W.; Wen, Z.; Jia, B.; Wang, L.; Jin, W.; Ma, T. Engineering Bismuth-Tin Interface in Bimetallic Aerogel with a 3D Porous Structure for Highly Selective Electrocatalytic CO_2 Reduction to HCOOH. *Angew. Chem.* **2021**, *133* (22), 12662−12667.
(67) Chen, B.; Wang, D.; Zhang, B.; Zhong, X.; Liu, Y.; Sheng, J.; Zhang, Q.; Zou, X.; Zhou, G.; Cheng, H. M. Engineering the Active Sites of Graphene Catalyst: From CO_2 Activation to Activate Li-CO_2 Batteries. *ACS Nano* **2021**, *15* (6), 9841−9850.
(68) Xiao, Y.; Du, F.; Hu, C.; Ding, Y.; Wang, Z. L.; Roy, A.; Dai, L. High-Performance Li-CO_2 Batteries from Free-Standing, Binder-Free, Bifunctional Three-Dimensional Carbon Catalysts. *ACS Energy Lett.* **2020**, *5* (3), 916−921.
(69) Feng, N.; He, P.; Zhou, H. Critical Challenges in Rechargeable Aprotic Li-O 2 Batteries. *Adv. Energy Mater.* **2016**, *6* (9), 1502303.
(70) Yang, C.; Guo, K.; Yuan, D.; Cheng, J.; Wang, B. Unraveling Reaction Mechanisms of Mo 2 C as Cathode Catalyst in a Li-CO_2 Battery. *J. Am. Chem. Soc.* **2020**, *142* (15), 6983−6990.
(71) Li, X.; Zhou, J.; Zhang, J.; Li, M.; Bi, X.; Liu, T.; He, T.; Cheng, J.; Zhang, F.; Li, Y.; Mu, X.; Lu, J.; Wang, B. Bamboo-Like Nitrogen-Doped Carbon Nanotube Forests as Durable Metal-Free Catalysts for Self-Powered Flexible Li-CO_2 Batteries. *Adv. Mater.* **2019**, *31* (39), 1903852.
(72) Ye, F.; Gong, L.; Long, Y.; Talapaneni, S. N.; Zhang, L.; Xiao, Y.; Liu, D.; Hu, C.; Dai, L. Topological Defect-Rich Carbon as a Metal-Free Cathode Catalyst for High-Performance Li-CO_2 Batteries. *Adv. Energy Mater.* **2021**, *11* (30), 2101390.

https://doi.org/10.1021/acsenergylett.2c02445
ACS Energy Lett. 2023, 8, 1818−1838

(73) Qiao, Y.; Wu, J.; Zhao, J.; Li, Q.; Zhang, P.; Hao, C.; Liu, X.; Yang, S.; Liu, Y. Synergistic Effect of Bifunctional Catalytic Sites and Defect Engineering for High-Performance Li-CO_2 Batteries. *Energy Storage Mater.* **2020**, *27*, 133−139.
(74) Hu, X.; Sun, J.; Li, Z.; Zhao, Q.; Chen, C.; Chen, J. Rechargeable Room-Temperature Na-CO_2 Batteries. *Angew. Chemie - Int. Ed.* **2016**, *55* (22), 6482−6486.
(75) Hu, X.; Joo, P. H.; Matios, E.; Wang, C.; Luo, J.; Yang, K.; Li, W. Designing an All-Solid-State Sodium-Carbon Dioxide Battery Enabled by Nitrogen-Doped Nanocarbon. *Nano Lett.* **2020**, *20* (5), 3620−3626.
(76) Daiyan, R.; Tan, X.; Chen, R.; Saputera, W. H.; Tahini, H. A.; Lovell, E.; Ng, Y. H.; Smith, S. C.; Dai, L.; Lu, X.; Amal, R. Electroreduction of CO_2 to CO on a Mesoporous Carbon Catalyst with Progressively Removed Nitrogen Moieties. *ACS Energy Lett.* **2018**, *3* (9), 2292−2298.
(77) Hu, C.; Bai, S.; Gao, L.; Liang, S.; Yang, J.; Cheng, S. D.; Mi, S. B.; Qiu, J. Porosity-Induced High Selectivity for CO_2 Electroreduction to CO on Fe-Doped ZIF-Derived Carbon Catalysts. *ACS Catal.* **2019**, *9* (12), 11579−11588.
(78) Li, C.; Wang, Y.; Xiao, N.; Li, H.; Ji, Y.; Guo, Z.; Liu, C.; Qiu, J. Nitrogen-Doped Porous Carbon from Coal for High Efficiency CO_2 Electrocatalytic Reduction. *Carbon N. Y.* **2019**, *151*, 46−52.
(79) Ni, W.; Xue, Y.; Zang, X.; Li, C.; Wang, H.; Yang, Z.; Yan, Y.-M. Fluorine Doped Cagelike Carbon Electrocatalyst: An Insight into the Structure-Enhanced CO Selectivity for CO_2 Reduction at High Overpotential. *ACS Nano* **2020**, *14* (2), 2014−2023.
(80) Ling, L.; Jiao, L.; Liu, X.; Dong, Y.; Yang, W.; Zhang, H.; Ye, B.; Chen, J.; Jiang, H. Potassium-Assisted Fabrication of Intrinsic Defects in Porous Carbons for Electrocatalytic CO_2 Reduction. *Adv. Mater.* **2022**, *34*, 2205933.
(81) Xue, D.; Xia, H.; Yan, W.; Zhang, J.; Mu, S. Defect Engineering on Carbon-Based Catalysts for Electrocatalytic CO_2 Reduction. *Nano-Micro Lett.* **2021**, *13* (1), 5.
(82) Guo, C.; Guo, Y.; Shi, Y.; Lan, X.; Wang, Y.; Yu, Y.; Zhang, B. Electrocatalytic Reduction of CO_2 to Ethanol at Close to Theoretical Potential via Engineering Abundant Electron-Donating Cu δ + Species. *Angew. Chem.* **2022**, *134* (32), 2−6.
(83) Li, M.; Idros, M. N.; Wu, Y.; Burdyny, T.; Garg, S.; Zhao, X. S.; Wang, G.; Rufford, T. E. The Role of Electrode Wettability in Electrochemical Reduction of Carbon Dioxide. *J. Mater. Chem. A* **2021**, *9* (35), 19369−19409.
(84) Bie, S.; Du, M.; He, W.; Zhang, H.; Yu, Z.; Liu, J.; Liu, M.; Yan, W.; Zhou, L.; Zou, Z. Carbon Nanotube@RuO 2 as a High Performance Catalyst for Li-CO_2 Batteries. *ACS Appl. Mater. Interfaces* **2019**, *11* (5), 5146−5151.
(85) Zhai, Y.; Tong, H.; Deng, J.; Li, G.; Hou, Y.; Zhang, R.; Wang, J.; Lu, Y.; Liang, K.; Chen, P.; Dang, F.; Kong, B. Super-Assembled Atomic Ir Catalysts on Te Substrates with Synergistic Catalytic Capability for Li-CO_2 Batteries. *Energy Storage Mater.* **2021**, *43* (May), 391−401.
(86) Guo, Z.; Li, J.; Qi, H.; Sun, X.; Li, H.; Tamirat, A. G.; Liu, J.; Wang, Y.; Wang, L. A Highly Reversible Long-Life Li-CO_2 Battery with a RuP 2 -Based Catalytic Cathode. *Small* **2019**, *15* (29), 1803246.
(87) Zhang, N.; Zhang, X.; Kang, Y.; Ye, C.; Jin, R.; Yan, H.; Lin, R.; Yang, J.; Xu, Q.; Wang, Y.; Zhang, Q.; Gu, L.; Liu, L.; Song, W.; Liu, J.; Wang, D.; Li, Y. A Supported Pd 2 Dual-Atom Site Catalyst for Efficient Electrochemical CO_2 Reduction. *Angew. Chem.* **2021**, *133* (24), 13500−13505.
(88) Zhang, N.; Zhang, X.; Tao, L.; Jiang, P.; Ye, C.; Lin, R.; Huang, Z.; Li, A.; Pang, D.; Yan, H.; Wang, Y.; Xu, P.; An, S.; Zhang, Q.; Liu, L.; Du, S.; Han, X.; Wang, D.; Li, Y. Silver Single-Atom Catalyst for Efficient Electrochemical CO_2 Reduction Synthesized from Thermal Transformation and Surface Reconstruction. *Angew. Chemie - Int. Ed.* **2021**, *60* (11), 6170−6176.
(89) Huang, J.; Mensi, M.; Oveisi, E.; Mantella, V.; Buonsanti, R. Structural Sensitivities in Bimetallic Catalysts for Electrochemical CO_2 Reduction Revealed by Ag-Cu Nanodimers. *J. Am. Chem. Soc.* **2019**, *141* (6), 2490−2499.
(90) Li, Z.; Wu, R.; Zhao, L.; Li, P.; Wei, X.; Wang, J.; Chen, J. S.; Zhang, T. Metal-Support Interactions in Designing Noble Metal-Based Catalysts for Electrochemical CO_2 Reduction: Recent Advances and Future Perspectives. *Nano Res.* **2021**, *14* (11), 3795−3809.
(91) Zhang, J.; Yin, R.; Shao, Q.; Zhu, T.; Huang, X. Oxygen Vacancies in Amorphous InO x Nanoribbons Enhance CO_2 Adsorption and Activation for CO_2 Electroreduction. *Angew. Chemie - Int. Ed.* **2019**, *58* (17), 5609−5613.
(92) Sun, K.; Ji, Y.; Liu, Y.; Wang, Z. Synergies between Electronic and Geometric Effects of Mo-Doped Au Nanoparticles for Effective CO_2 electrochemical Reduction. *J. Mater. Chem. A* **2020**, *8* (25), 12291−12295.
(93) Zhou, J. H.; Yuan, K.; Zhou, L.; Guo, Y.; Luo, M. Y.; Guo, X. Y.; Meng, Q. Y.; Zhang, Y. W. Boosting Electrochemical Reduction of CO_2 at a Low Overpotential by Amorphous Ag-Bi-S-O Decorated Bi0 Nanocrystals. *Angew. Chemie - Int. Ed.* **2019**, *58* (40), 14197−14201.
(94) Gao, D.; Zhang, Y.; Zhou, Z.; Cai, F.; Zhao, X.; Huang, W.; Li, Y.; Zhu, J.; Liu, P.; Yang, F.; Wang, G.; Bao, X. Enhancing CO_2 Electroreduction with the Metal-Oxide Interface. *J. Am. Chem. Soc.* **2017**, *139* (16), 5652−5655.
(95) Chen, B.; Wang, D.; Tan, J.; Liu, Y.; Jiao, M.; Liu, B.; Zhao, N.; Zou, X.; Zhou, G.; Cheng, H.-M. Designing Electrophilic and Nucleophilic Dual Centers in the ReS_2 Plane toward Efficient Bifunctional Catalysts for Li-CO_2 Batteries. *J. Am. Chem. Soc.* **2022**, *144* (7), 3106−3116.
(96) Cai, Y.; Fu, J.; Zhou, Y.; Chang, Y.-C.; Min, Q.; Zhu, J.-J.; Lin, Y.; Zhu, W. Insights on Forming N,O-Coordinated Cu Single-Atom Catalysts for Electrochemical Reduction CO_2 to Methane. *Nat. Commun.* **2021**, *12* (1), 586.
(97) Li, L.; Ozden, A.; Guo, S.; Garcıa de Arquer, F. P.; Wang, C.; Zhang, M.; Zhang, J.; Jiang, H.; Wang, W.; Dong, H.; Sinton, D.; Sargent, E. H.; Zhong, M. Stable, Active CO_2 Reduction to Formate via Redox-Modulated Stabilization of Active Sites. *Nat. Commun.* **2021**, *12* (1), 5223.
(98) Marcandalli, G.; Goyal, A.; Koper, M. T. M. Electrolyte Effects on the Faradaic Efficiency of CO_2 Reduction to CO on a Gold Electrode. *ACS Catal.* **2021**, *11* (9), 4936−4945.
(99) Pipes, R.; Bhargav, A.; Manthiram, A. Nanostructured Anatase Titania as a Cathode Catalyst for Li-CO_2 Batteries. *ACS Appl. Mater. Interfaces* **2018**, *10* (43), 37119−37124.
(100) Hou, Y.; Wang, J.; Liu, L.; Liu, Y.; Chou, S.; Shi, D.; Liu, H.; Wu, Y.; Zhang, W.; Chen, J. Mo 2 C/CNT: An Efficient Catalyst for Rechargeable Li-CO_2 Batteries. *Adv. Funct. Mater.* **2017**, *27* (27), 1700564.
(101) Yang, C.; Guo, K.; Yuan, D.; Cheng, J.; Wang, B. Unraveling Reaction Mechanisms of Mo2C as Cathode Catalyst in a Li-CO_2 Battery. *J. Am. Chem. Soc.* **2020**, *142* (15), 6983−6990.
(102) Pichaimuthu, K.; Jena, A.; Chang, H.; Su, C.; Hu, S. F.; Liu, R. S. Molybdenum Disulfide/Tin Disulfide Ultrathin Nanosheets as Cathodes for Sodium-Carbon Dioxide Batteries. *ACS Appl. Mater. Interfaces* **2022**, *14* (4), 5834−5842.
(103) Ge, B.; Sun, Y.; Guo, J.; Yan, X.; Fernandez, C.; Peng, Q. A Co-Doped MnO_2 Catalyst for Li-CO_2 Batteries with Low Overpotential and Ultrahigh Cyclability. *Small* **2019**, *15* (34), 1902220.
(104) Xu, C.; Wang, H.; Zhan, J.; Kang, Y.; Liang, F. Engineering NH3-Induced 1D Self-Assembly Architecture with Conductive Polymer for Advanced Hybrid Na-CO_2 Batteries via Morphology Modulation. *J. Power Sources* **2022**, *520*, 230909.
(105) Wang, J.; Gan, L.; Zhang, Q.; Reddu, V.; Peng, Y.; Liu, Z.; Xia, X.; Wang, C.; Wang, X. A Water-Soluble Cu Complex as Molecular Catalyst for Electrocatalytic CO_2 Reduction on Graphene-Based Electrodes. *Adv. Energy Mater.* **2019**, *9* (3), 1803151.
(106) Franco, F.; Rettenmaier, C.; Jeon, H. S.; Roldan Cuenya, B. Transition Metal-Based Catalysts for the Electrochemical CO_2 reduction: From Atoms and Molecules to Nanostructured Materials. *Chem. Soc. Rev.* **2020**, *49* (19), 6884−6946.
(107) Wang, Y.; Wang, W.; Xie, J.; Wang, C. H.; Yang, Y. W.; Lu, Y. C. Electrochemical Reduction of CO_2 in Ionic Liquid: Mechanistic Study of Li-CO_2 Batteries via in Situ Ambient Pressure X-Ray Photoelectron Spectroscopy. *Nano Energy* **2021**, *83*, 105830.

https://doi.org/10.1021/acsenergylett.2c02445
ACS Energy Lett. 2023, 8, 1818−1838

(108) Xu, C.; Zhan, J.; Wang, H.; Kang, Y.; Liang, F. Dense Binary Fe-Cu Sites Promoting CO_2 utilization Enable Highly Reversible Hybrid Na-CO_2 batteries. *J. Mater. Chem. A* **2021**, *9* (38), 22114−22128.
(109) Zheng, W.; Wang, Y.; Shuai, L.; Wang, X.; He, F.; Lei, C.; Li, Z.; Yang, B.; Lei, L.; Yuan, C.; Qiu, M.; Hou, Y.; Feng, X. Highly Boosted Reaction Kinetics in Carbon Dioxide Electroreduction by Surface-Introduced Electronegative Dopants. *Adv. Funct. Mater.* **2021**, *31* (15), 2008146.
(110) Ni, W.; Liu, Z.; Zhang, Y.; Ma, C.; Deng, H.; Zhang, S.; Wang, S. Electroreduction of Carbon Dioxide Driven by the Intrinsic Defects in the Carbon Plane of a Single Fe-N 4 Site. *Adv. Mater.* **2021**, *33* (1), 2003238.
(111) Wang, T.; Sang, X.; Zheng, W.; Yang, B.; Yao, S.; Lei, C.; Li, Z.; He, Q.; Lu, J.; Lei, L.; Dai, L.; Hou, Y. Gas Diffusion Strategy for Inserting Atomic Iron Sites into Graphitized Carbon Supports for Unusually High-Efficient CO_2 Electroreduction and High-Performance Zn-CO_2 Batteries. *Adv. Mater.* **2020**, *32* (29), 2002430.
(112) Li, Z.; Jiang, J.; Liu, X.; Zhu, Z.; Wang, J.; He, Q.; Kong, Q.; Niu, X.; Chen, J. S.; Wang, J.; Wu, R. Coupling Atomically Dispersed Fe-N 5 Sites with Defective N-Doped Carbon Boosts CO_2 Electroreduction. *Small* **2022**, *18* (38), 2203495.
(113) Chen, J.; Li, Z.; Wang, X.; Sang, X.; Zheng, S.; Liu, S.; Yang, B.; Zhang, Q.; Lei, L.; Dai, L.; Hou, Y. Promoting CO_2 Electroreduction Kinetics on Atomically Dispersed Monovalent Zn I Sites by Rationally Engineering Proton-Feeding Centers. *Angew. Chem.* **2022**, *134* (7), e202111683 DOI: 10.1002/ange.202111683.
(114) Lian, Z.; Lu, Y.; Wang, C.; Zhu, X.; Ma, S.; Li, Z.; Liu, Q.; Zang, S. Single-Atom Ru Implanted on Co 3 O 4 Nanosheets as Efficient Dual-Catalyst for Li-CO_2 Batteries. *Adv. Sci.* **2021**, *8* (23), 2102550.
(115) Jiao, L.; Zhu, J.; Zhang, Y.; Yang, W.; Zhou, S.; Li, A.; Xie, C.; Zheng, X.; Zhou, W.; Yu, S. H.; Jiang, H. L. Non-Bonding Interaction of Neighboring Fe and Ni Single-Atom Pairs on MOF-Derived N-Doped Carbon for Enhanced CO_2 Electroreduction. *J. Am. Chem. Soc.* **2021**, *143* (46), 19417−19424.
(116) Zhang, Z.; Bai, W.; Cai, Z.; Cheng, J.; Kuang, H.; Dong, B.; Wang, Y.; Wang, K.; Chen, J. Enhanced Electrochemical Performance of Aprotic Li-CO_2 Batteries with a Ruthenium-Complex-Based Mobile Catalyst. *Angew. Chem.* **2021**, *133* (30), 16540−16544.
(117) Qi, G.; Zhang, J.; Chen, L.; Wang, B.; Cheng, J. Binder-Free MoN Nanofibers Catalysts for Flexible 2-Electron Oxalate-Based Li-CO_2 Batteries with High Energy Efficiency. *Adv. Funct. Mater.* **2022**, *32* (22), 2112501.
(118) Gao, S.; Jin, M.; Sun, J.; Liu, X.; Zhang, S.; Li, H.; Luo, J.; Sun, X. Coralloid Au Enables High-Performance Zn-CO_2 Battery and Self-Driven CO Production. *J. Mater. Chem. A* **2021**, *9* (37), 21024−21031.
(119) Hao, J.; Zhuang, Z.; Hao, J.; Cao, K.; Hu, Y.; Wu, W.; Lu, S.; Wang, C.; Zhang, N.; Wang, D.; Du, M.; Zhu, H. Strain Relaxation in Metal Alloy Catalysts Steers the Product Selectivity of Electrocatalytic CO_2 Reduction. *ACS Nano* **2022**, *16* (2), 3251−3263.
(120) Zhang, E.; Wang, T.; Yu, K.; Liu, J.; Chen, W.; Li, A.; Rong, H.; Lin, R.; Ji, S.; Zheng, X.; Wang, Y.; Zheng, L.; Chen, C.; Wang, D.; Zhang, J.; Li, Y. Bismuth Single Atoms Resulting from Transformation of Metal-Organic Frameworks and Their Use as Electrocatalysts for CO_2 Reduction. *J. Am. Chem. Soc.* **2019**, *141* (42), 16569−16573.
(121) Jiang, Z.; Wang, T.; Pei, J.; Shang, H.; Zhou, D.; Li, H.; Dong, J.; Wang, Y.; Cao, R.; Zhuang, Z.; Chen, W.; Wang, D.; Zhang, J.; Li, Y. Discovery of Main Group Single Sb-N4active Sites for CO_2 electroreduction to Formate with High Efficiency. *Energy Environ. Sci.* **2020**, *13* (9), 2856−2863.
(122) Zheng, T.; Jiang, K.; Ta, N.; Hu, Y.; Zeng, J.; Liu, J.; Wang, H. Large-Scale and Highly Selective CO_2 Electrocatalytic Reduction on Nickel Single-Atom Catalyst. *Joule* **2019**, *3* (1), 265−278.
(123) Xiong, W.; Li, H.; Wang, H.; Yi, J.; You, H.; Zhang, S.; Hou, Y.; Cao, M.; Zhang, T.; Cao, R. Hollow Mesoporous Carbon Sphere Loaded Ni-N 4 Single-Atom: Support Structure Study for CO_2 Electrocatalytic Reduction Catalyst. *Small* **2020**, *16* (41), 2003943.
(124) Zhang, H.; Li, J.; Xi, S.; Du, Y.; Hai, X.; Wang, J.; Xu, H.; Wu, G.; Zhang, J.; Lu, J.; Wang, J. A Graphene-Supported Single-Atom FeN 5 Catalytic Site for Efficient Electrochemical CO_2 Reduction. *Angew. Chem.* **2019**, *131* (42), 15013−15018.
(125) Lin, J.; Ding, J.; Wang, H.; Yang, X.; Zheng, X.; Huang, Z.; Song, W.; Ding, J.; Han, X.; Hu, W. Boosting Energy Efficiency and Stability of Li-CO_2 Batteries via Synergy between Ru Atom Clusters and Single-Atom Ru-N 4 Sites in the Electrocatalyst Cathode. *Adv. Mater.* **2022**, *34* (17), 2200559.
(126) Zhan, C.; Dattila, F.; Rettenmaier, C.; Bergmann, A.; Kühl, S.; García-Muelas, R.; López, N.; Cuenya, B. R. Revealing the CO Coverage-Driven C-C Coupling Mechanism for Electrochemical CO_2 Reduction on Cu2O Nanocubesvia OperandoRaman Spectroscopy. *ACS Catal.* **2021**, *11* (13), 7694−7701.
(127) Han, J.; An, P.; Liu, S.; Zhang, X.; Wang, D.; Yuan, Y.; Guo, J.; Qiu, X.; Hou, K.; Shi, L.; Zhang, Y.; Zhao, S.; Long, C.; Tang, Z. Reordering d Orbital Energies of Single-Site Catalysts for CO_2 Electroreduction. *Angew. Chem.* **2019**, *131* (36), 12841−12846.
(128) Yang, F.; Hu, W.; Yang, C.; Patrick, M.; Cooksy, A. L.; Zhang, J.; Aguiar, J. A.; Fang, C.; Zhou, Y.; Meng, Y. S.; Huang, J.; Gu, J. Tuning Internal Strain in Metal-Organic Frameworks via Vapor Phase Infiltration for CO_2 Reduction. *Angew. Chem.* **2020**, *132* (11), 4602−4610.
(129) Du, J.; Lang, Z.-L.; Ma, Y.-Y.; Tan, H.-Q.; Liu, B.-L.; Wang, Y.-H.; Kang, Z.-H.; Li, Y.-G. Polyoxometalate-Based Electron Transfer Modulation for Efficient Electrocatalytic Carbon Dioxide Reduction. *Chem. Sci.* **2020**, *11* (11), 3007−3015.
(130) Gong, S.; Wang, W.; Zhang, C.; Zhu, M.; Lu, R.; Ye, J.; Yang, H.; Wu, C.; Liu, J.; Rao, D.; Shao, S.; Lv, X. Tuning the Metal Electronic Structure of Anchored Cobalt Phthalocyanine via Dual-Regulator for Efficient CO_2 Electroreduction and Zn-CO_2 Batteries. *Adv. Funct. Mater.* **2022**, *32* (17), 2110649.
(131) Chen, J.; Zou, K.; Ding, P.; Deng, J.; Zha, C.; Hu, Y.; Zhao, X.; Wu, J.; Fan, J.; Li, Y. Conjugated Cobalt Polyphthalocyanine as the Elastic and Reprocessable Catalyst for Flexible Li-CO_2 Batteries. *Adv. Mater.* **2019**, *31* (2), 1805484.
(132) Dou, S.; Song, J.; Xi, S.; Du, Y.; Wang, J.; Huang, Z.; Xu, Z. J.; Wang, X. Boosting Electrochemical CO_2 Reduction on Metal-Organic Frameworks via Ligand Doping. *Angew. Chemie Int. Ed.* **2019**, *58* (12), 4041−4045.
(133) Li, S.; Dong, Y.; Zhou, J.; Liu, Y.; Wang, J.; Gao, X.; Han, Y.; Qi, P.; Wang, B. Carbon Dioxide in the Cage: Manganese Metal-Organic Frameworks for High Performance CO_2 Electrodes in Li-CO_2 Batteries. *Energy Environ. Sci.* **2018**, *11* (5), 1318−1325.
(134) Li, X.; Wang, H.; Chen, Z.; Xu, H.; Yu, W.; Liu, C.; Wang, X.; Zhang, K.; Xie, K.; Loh, K. P. Covalent-Organic-Framework-Based Li-CO_2 Batteries. *Adv. Mater.* **2019**, *31* (48), 1905879.
(135) Shimoni, R.; Shi, Z.; Binyamin, S.; Yang, Y.; Liberman, I.; Ifraemov, R.; Mukhopadhyay, S.; Zhang, L.; Hod, I. Electrostatic Secondary-Sphere Interactions That Facilitate Rapid and Selective Electrocatalytic CO_2 Reduction in a Fe-Porphyrin-Based Metal-Organic Framework. *Angew. Chem.* **2022**, *134* (32), e202206085 DOI: 10.1002/ange.202206085.
(136) Guo, Y.; Shi, W.; Yang, H.; He, Q.; Zeng, Z.; Ye, J. Y.; He, X.; Huang, R.; Wang, C.; Lin, W. Cooperative Stabilization of the [Pyridinium-CO_2 -Co] Adduct on a Metal-Organic Layer Enhances Electrocatalytic CO_2 Reduction. *J. Am. Chem. Soc.* **2019**, *141* (44), 17875−17883.
(137) Al-Attas, T. A.; Marei, N. N.; Yong, X.; Yasri, N. G.; Thangadurai, V.; Shimizu, G.; Siahrostami, S.; Kibria, M. G. Ligand-Engineered Metal-Organic Frameworks for Electrochemical Reduction of Carbon Dioxide to Carbon Monoxide. *ACS Catal.* **2021**, *11* (12), 7350−7357.
(138) Leverett, J.; Tran-Phu, T.; Yuwono, J. A.; Kumar, P.; Kim, C.; Zhai, Q.; Han, C.; Qu, J.; Cairney, J.; Simonov, A. N.; Hocking, R. K.; Dai, L.; Daiyan, R.; Amal, R. Tuning the Coordination Structure of Cu−N−C Single Atom Catalysts for Simultaneous Electrochemical Reduction of CO_2 and NO_3 - to Urea. *Adv. Energy Mater.* **2022**, *12* (32), 2201500.

(139) Wang, J.; Xu, F.; Wang, Z.; Zang, S.; Mak, T. C. W. Ligand-Shell Engineering of a Au 28 Nanocluster Boosts Electrocatalytic CO_2 Reduction. *Angew. Chem.* **2022**, *134* (32), 1−6.
(140) Zhuo, L.; Chen, P.; Zheng, K.; Zhang, X.; Wu, J.; Lin, D.; Liu, S.; Wang, Z.; Liu, J.; Zhou, D.; Zhang, J. Flexible Cuprous Triazolate Frameworks as Highly Stable and Efficient Electrocatalysts for CO_2 Reduction with Tunable C 2 H 4 /CH 4 Selectivity. *Angew. Chem.* **2022**, *134* (28), 1−5.
(141) Chen, J.; Wang, L. Effects of the Catalyst Dynamic Changes and Influence of the Reaction Environment on the Performance of Electrochemical CO_2 Reduction. *Adv. Mater.* **2022**, *34* (25), 2103900.
(142) Wang, J.; Zheng, X.; Wang, G.; Cao, Y.; Ding, W.; Zhang, J.; Wu, H.; Ding, J.; Hu, H.; Han, X.; Ma, T.; Deng, Y.; Hu, W. Defective Bimetallic Selenides for Selective CO_2 Electroreduction to CO. *Adv. Mater.* **2022**, *34* (3), 2106354.
(143) Zhong, M.; Tran, K.; Min, Y.; Wang, C.; Wang, Z.; Dinh, C.-T.; De Luna, P.; Yu, Z.; Rasouli, A. S.; Brodersen, P.; Sun, S.; Voznyy, O.; Tan, C.-S.; Askerka, M.; Che, F.; Liu, M.; Seifitokaldani, A.; Pang, Y.; Lo, S.-C.; Ip, A.; Ulissi, Z.; Sargent, E. H. Accelerated Discovery of CO_2 Electrocatalysts Using Active Machine Learning. *Nature* **2020**, *581* (7807), 178−183.
(144) Zhang, N.; Yang, B.; Liu, K.; Li, H.; Chen, G.; Qiu, X.; Li, W.; Hu, J.; Fu, J.; Jiang, Y.; Liu, M.; Ye, J. Machine Learning in Screening High Performance Electrocatalysts for CO_2 Reduction. *Small Methods* **2021**, *5* (11), 2100987.
(145) Zhao, S.; Yang, Y.; Tang, Z. Insight into Structural Evolution, Active Sites, and Stability of Heterogeneous Electrocatalysts. *Angew. Chem.* **2022**, *134* (11), e202110186 DOI: 10.1002/ange.202110186.
(146) Thoka, S.; Tong, Z.; Jena, A.; Hung, T.-F.; Wu, C.-C.; Chang, W.-S.; Wang, F.-M.; Wang, X.-C.; Yin, L.-C.; Chang, H.; Hu, S.-F.; Liu, R.-S. High-Performance Na-CO_2 Batteries with ZnCo 2 O 4 @CNT as the Cathode Catalyst. *J. Mater. Chem. A* **2020**, *8* (45), 23974−23982.
(147) Zhang, Y.; Jiao, L.; Yang, W.; Xie, C.; Jiang, H. Rational Fabrication of Low-Coordinate Single-Atom Ni Electrocatalysts by MOFs for Highly Selective CO_2 Reduction. *Angew. Chemie Int. Ed.* **2021**, *60* (14), 7607−7611.
(148) Liu, H.; Liu, J.; Yang, B. Promotional Role of a Cation Intermediate Complex in C2Formation from Electrochemical Reduction of CO_2 over Cu. *ACS Catal.* **2021**, *11* (19), 12336−12343.
(149) Liu, X.; Schlexer, P.; Xiao, J.; Ji, Y.; Wang, L.; Sandberg, R. B.; Tang, M.; Brown, K. S.; Peng, H.; Ringe, S.; Hahn, C.; Jaramillo, T. F.; Nørskov, J. K.; Chan, K. PH Effects on the Electrochemical Reduction of CO(2) towards C2 Products on Stepped Copper. *Nat. Commun.* **2019**, *10* (1), 32.
(150) Rotundo, L.; Filippi, J.; Gobetto, R.; Miller, H. A.; Rocca, R.; Nervi, C.; Vizza, F. Electrochemical CO_2 Reduction in Water at Carbon Cloth Electrodes Functionalized with a Fac-Mn(Apbpy)(CO)3Br Complex. *Chem. Commun.* **2019**, *55* (6), 775−777.

https://doi.org/10.1021/acsenergylett.2c02445
ACS Energy Lett. 2023, 8, 1818−1838